Journal of Hazardous Materials 419 (2021) 126378

Contents lists available at ScienceDirect

Journal of Hazardous Materials

journal homepage: www.elsevier.com/locate/jhazmat

Cobalt induces neurodegenerative damages through Pin1 inactivation in mice and human neuroglioma cells

Fuli Zheng [a,b,c,1], Yuqing Li [a,1], Fengshun Zhang [a], Yi Sun [d], Chunyan Zheng [a], Zhousong Luo [a], Yuan-Liang Wang [a,b,c], Michael Aschner [e], Hong Zheng [f], Liqiong Lin [f], Ping Cai [b,c,g], Wenya Shao [a,b,c], Zhenkun Guo [b,c], Min Zheng [h], Xiao Zhen Zhou [i], Kun Ping Lu [i], Siying Wu [b,c,d,*], Huangyuan Li [a,b,c,*]

[a] Department of Preventive Medicine, School of Public Health, Fujian Medical University, Fuzhou 350122, China
[b] Fujian Provincial Key Laboratory of Environmental Factors and Cancer, School of Public Health, Fujian Medical University, Fuzhou 350122, China
[c] The Key Laboratory of Environment and Health, School of Public Health, Fujian Medical University, Fuzhou 350122, China
[d] Department of Epidemiology and Health Statistics, School of Public Health, Fujian Medical University, Fuzhou 350122, China
[e] Department of Molecular Pharmacology, Albert Einstein College of Medicine, 1300 Morris Park Avenue, Bronx, NY 10461, USA
[f] Fuzhou Second Hospital Affiliated to Xiamen University, Fuzhou 350007, China
[g] Department of Health Inspection and Quarantine, School of Public Health, Fujian Medical University, Fuzhou 350122, China
[h] Institute for Translational Medicine, Fujian Medical University, Fuzhou 350122, China
[i] Division of Translational Therapeutics, Department of Medicine, Beth Israel Deaconess Medical Center, Harvard Medical School, Boston, MA 02215, USA

ARTICLE INFO

Editor: Dr. S.Y. Chen

Keywords:
Cobalt
Pin1
Neurodegeneration
Phosphorylated Tau (P-Tau)

ABSTRACT

Cobalt is a hazardous material that has harmful effects on neurotoxicity. Excessive exposure to cobalt or inactivation of the unique proline isomerase Pin1 contributes to age-dependent neurodegeneration. However, nothing is known about the role of Pin1 in cobalt-induced neurodegeneration. Here we find that out of several hazardous materials, only cobalt dose-dependently decreased Pin1 expression and alterations in its substrates, including *cis* and *trans* phosphorylated Tau in human neuronal cells, concomitant with neurotoxicity. Cobalt-induced neurotoxicity was aggravated by Pin1 genetic or chemical inhibition, but rescued by Pin1 upregulation. Furthermore, less than 4 μg/l of blood cobalt induced dose- and age-dependent Pin1 downregulation in murine brains, ensuing neurodegenerative changes. These defects were corroborated by changes in Pin1 substrates, including *cis* and *trans* phosphorylated Tau, amyloid precursor protein, β amyloid and GSK3β. Moreover, blood Pin1 was downregulated in human hip replacement patients with median blood cobalt level of 2.514 μg/l, which is significantly less than the safety threshold of 10 μg/l, suggesting an early role Pin1 played in neurodegenerative damages. Thus, Pin1 inactivation by cobalt contributes to age-dependent neurodegeneration, revealing that cobalt is a hazardous material triggering AD-like neurodegenerative damages.

1. Introduction

Cobalt and its compounds are widely distributed in nature and globally used in industries, including batteries, hard alloys, magnetic materials, catalysts, desiccants, reagents, pigments and dyes. As a component of vitamin B_{12}, cobalt is an essential element for cellular growth, differentiation and development (Bumoko et al., 2015; Deshmukh et al., 2013). However, excessive bodily cobalt can cause toxicity (Fowler, 2016; Lison et al., 2018). It is characterized by cognitive deficits, neuritis, sensorineural deafness, neurological tinnitus, optic atrophy, visual impairment due to occupational, environmental, dietary exposure or endogenous release from cobalt alloy artificial prostheses (joint replacement) (Catalani et al., 2012a; Leyssens et al., 2017). More than 1 million metal-on-metal (MoM) articulations have been implanted worldwide, leading it one of the most important cobalt exposure sources (Tvermoes et al., 2015; Bozic, 2009). The majority of patients with

* Corresponding authors at: Fujian Provincial Key Laboratory of Environmental Factors and Cancer, School of Public Health, Fujian Medical University, Fuzhou 350122, China
E-mail addresses: sywu@fjmu.edu.cn (S. Wu), fmulhy@163.com, lhy@fjmu.edu.cn (H. Li).
[1] These authors contributed equally to this work.

https://doi.org/10.1016/j.jhazmat.2021.126378
Received 7 April 2021; Received in revised form 29 May 2021; Accepted 8 June 2021
Available online 12 June 2021

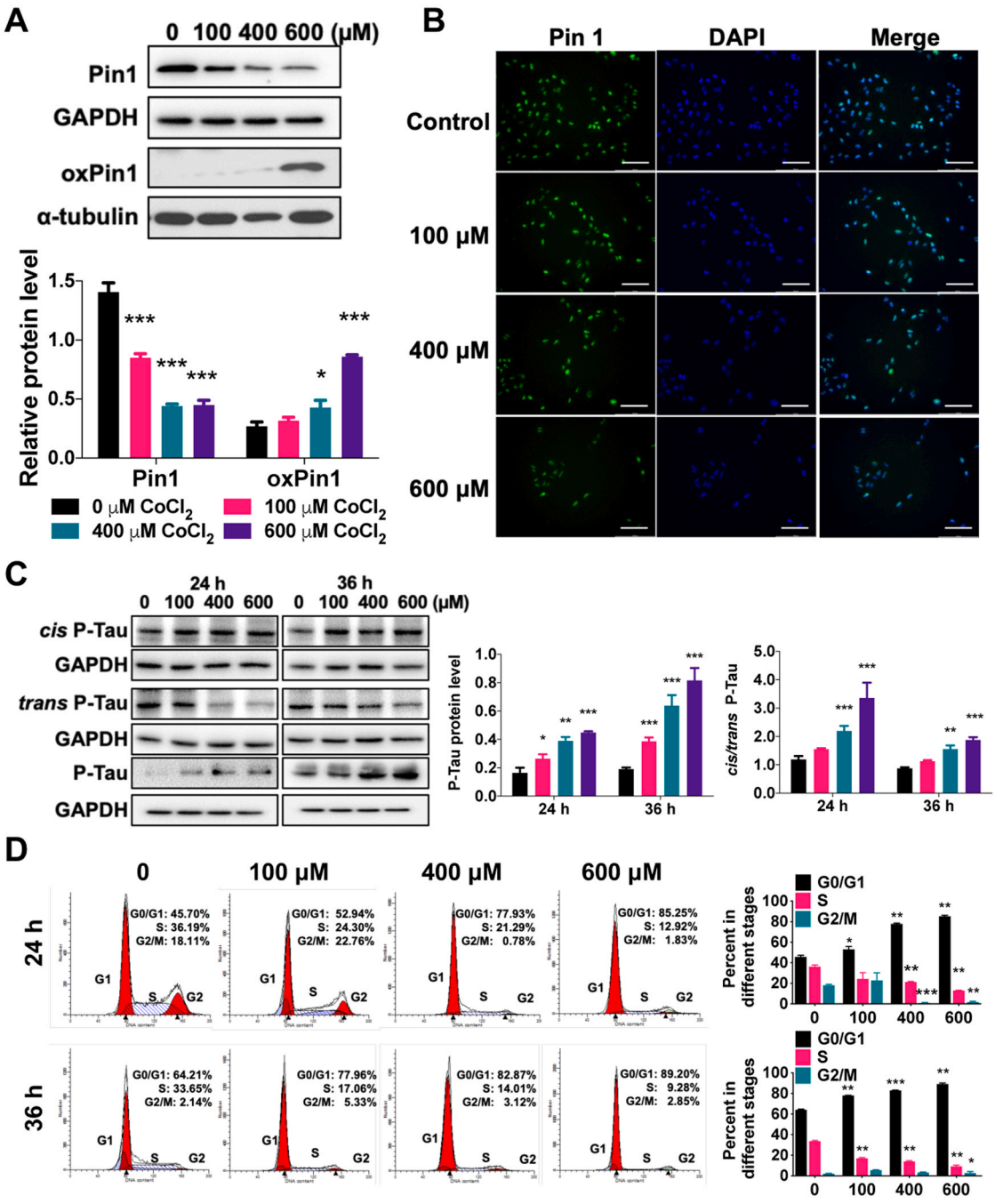

Fig. 1. Effects on Pin1 expression and cytotoxicity upon $CoCl_2$ exposure. (A) After 36 h exposure to $CoCl_2$, Pin1 protein level was decreased concomitant with upregulation of the oxidative form of Pin1 (oxPin1), the inactive form of Pin1. (B) Pin1 protein level was also detected with fluorescent microscopy (green) after 36 h $CoCl_2$ exposure. DAPI (blue) labels nuclei. (C) Cobalt increased the ratio of *cis/trans* P-Tau and T231 P-Tau after 24 h and 36 h exposure in a concentration-dependent manner, suggesting the inactivation of Pin1 isomerase activity upon cobalt exposure. (D) $CoCl_2$ caused cell cycle arrest in the G0/G1 phase after 24 h and 36 h exposure. Apoptotic rates increased in response to $CoCl_2$ exposure as noted by Hoechst staining (E) and Annexin V/PI-flow cytometry (F). (G) Corroborating to the cell cycle arrest and apoptosis, Cyclin D1 was downregulated, while Caspase-9 protein level was upregulated after 24 h and 36 h $CoCl_2$ exposure. $^{*}P < 0.05$, $^{**}P < 0.01$ and $^{***}P < 0.001$ compared with the control (0 μM $CoCl_2$). Scale bar for (B): 100 μm; (E): 500 μm. (For interpretation of the references to colour in this figure legend, the reader is referred to the web version of this article.)

well-functioning implants have blood cobalt concentrations ranging between 0.2 and 10 μg/l (Leyssens et al., 2017). *In vivo* and *in vitro* studies have shown that excess cobalt causes reduction in exploratory behavior in rats, repression of synaptic transmission, and Aβ release from neuroblastoma (SHSY5Y) cells (Zheng et al., 2019; Olivieri et al., 2001a; Tang et al., 2020a). These results suggest a potential connection between cobalt and neurodegeneration. However, how cobalt contributes to neurodegeneration is not fully understood.

Notably, brain cobalt levels in patients with Alzheimer's disease have been shown to be 1.8 times higher than those in controls (Wenstrup et al., 1990). Alzheimer's disease (AD) is the most common neurodegenerative disease characterized by progressive cognitive function and memory disorder mostly found in the elderly. Accumulation of extracellular senile plaques composed of β amyloid (Aβ), intracellular

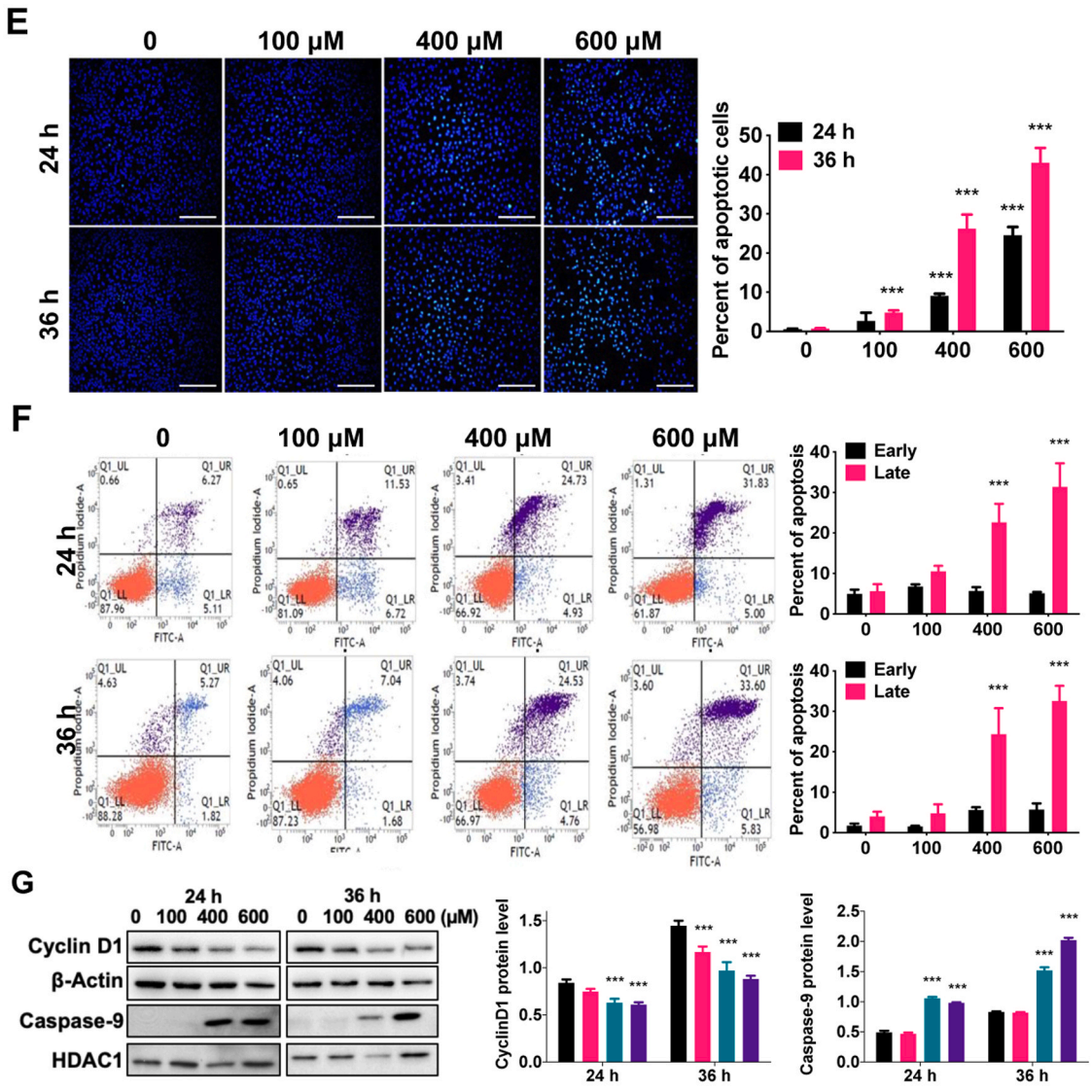

Fig. 1. (*continued*).

neurofibrillary tangles (NFT) composed of hyperphosphorylated Tau, and a progressive neuronal loss are distinct pathological features of AD (Mattson, 2004). Worldwide, approximately 50 million people suffer from AD-related dementia, with up to 82 million expected by 2030 and 152 million by 2050 (International AsD, 2019). Approximately 400 heritability studies have established that only about 10% of AD may be accounted for by heritability, the remaining 90% being due to environmental factors (Manolio et al., 2009). Heavy metals such as copper, zinc and iron are considered risk factors of neurodegenerative diseases, including AD (Bolognin et al., 2009).

Pin1 in the AD brain hippocampus is significantly reduced and/or oxidized to the inactive form (oxPin1), leading to loss of Pin1 isomerase activity (Sultana et al., 2006). Pin1 is a unique peptidyl-prolyl *cis-trans* isomerase (PPIase), which specifically isomerizes certain Ser/Thr-Pro motifs after phosphorylation, thereby regulating the function of the substrate protein (Lu et al., 1999). This conformational transformation mediated by Pin1 has profound effects on stress response, cell growth, neuronal differentiation, survival, immune function and germ cell development (Lu et al., 1999; Becker and Bonni, 2006). Furthermore, neurodegenerative changes have been observed in Pin1 knockout mice (Becker and Bonni, 2006). Pin1 SNP preventing Pin1 inhibition delays the onset of AD in humans (Ma et al., 2012) and a Pin1 loss-function somatic mutation is identified in human AD patients (Park et al., 2019). Pin1 has been shown to prevent neurodegeneration in AD by repressing extracellular senile plaque and intracellular NFTs accumulation by accelerating dephosphorylation of P-Tau and amyloid precursor protein (APP) (Sultana et al., 2006; Pastorino et al., 2006; Nakamura et al., 2012). When phosphorylated, Tau exists in two isoforms: pathological *cis* and physiological *trans*. The *trans* isoform is functional and undergoes dephosphorylation and degradation. In contrast, *cis* P-Tau is non-functional and cannot be dephosphorylated and degraded, with high tendency for aggregation and tangle formation. The *cis* P-Tau antibody has been proven beneficial for the detection of the 'toxic' version of Tau in early stages of AD (Kondo et al., 2015). These results indicate that Pin1 helps protect against age-dependent neurodegeneration in AD. However, so far nothing is known about whether cobalt alters Pin1 level and activity, and whether Pin1 plays any role in environmentally triggered AD.

Here, we investigated cobalt toxicity both *in vitro* and *in vivo* to address the interplay between cobalt exposure, age and Pin1 in triggering neurological dysfunction. The role of Pin1 was examined in human neuroglioma cells upon both genetic modification and chemical inhibition. As the population avoids the complexity and interference between mixed occupational exposure sources, the clinical significance of our findings was further substantiated by correlating the levels of cobalt and Pin1 in clinical human blood samples derived from hip

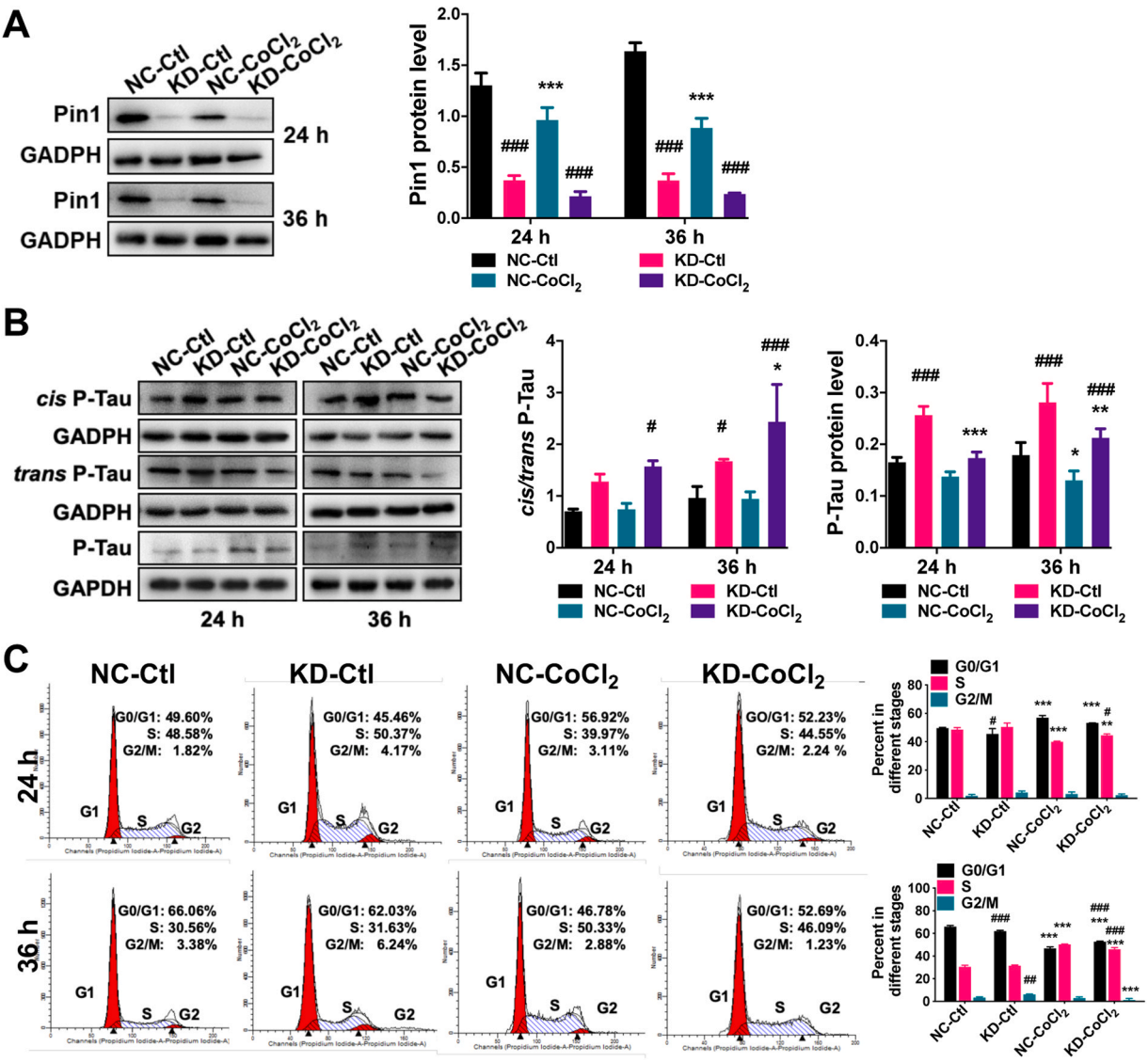

Fig. 2. Effects of cobalt on neurotoxicity in H4 cells with Pin1 knockdown. Pin1 knockdown (labeled as KD) cells were exposed for 24 or 36 h to 400 μM $CoCl_2$. (A) Pin1 was downregulated with a lentivirus knockdown vector. Cobalt exposure induced further reduction in Pin1 protein levels. (B) Protein expression of *cis* P-Tau, *trans* P-Tau and T231 P-Tau in response to $CoCl_2$. The ratio of *cis/trans* P-Tau is shown next to the western blot. (C) $CoCl_2$ led to cell cycle arrest in the G0/G1 phase after 24 h exposure and in the S phase after 36 h exposure. (D) Apoptosis rates, detected by Annexin V/ PI-flow cytometry, increased in response to $CoCl_2$ exposure. € Absent cobalt exposure, Pin1 KD cells viability was indistinguishable from controls. However, upon cobalt exposure, cell viability significantly decreased, as evidenced with the CCK-8 assay. Data represent mean ± SD (n = 6). (F) Cell cycle regulation protein Cyclin D1 was downregulated in H4 KD cells after 24 h or 36 h of $CoCl_2$ exposure. NC groups represent H4 cells transfected with control lentivirus, as a negative control of the Pin1 KD cells. $^{*}P < 0.05$, $^{**}P < 0.01$ and $^{***}P < 0.001$ when comparing between the presence and absence of cobalt under the same Pin1 condition (*i.e.*, within NC groups or KD groups); # $P < 0.05$, ## $P < 0.01$ and ### $P < 0.001$ when comparing between NC and Pin1 KD cells upon same exposures (either both exposed or unexposed to cobalt).

replacement patients with endogenous cobalt exposure.

2. Methods

2.1. Reagents

Cobalt (II) chloride hexahydrate (99.9% w/w) was purchased from Sigma-Aldrich (USA). Co^{2+} standard solution for ICP-MS was purchased from PerkinElmer (USA). TRIzol reagent was purchased from Invitrogen TM Life Technologies (USA). PrimeScript 1st Strand cDNA Synthesis Kit and *in situ* Apoptosis Detection Kit were purchased from Takara (Japan). Anti-GAPDH antibody, anti-Caspase-9 antibody, anti-Tau antibody, anti-Tau (phospho T231) antibody, anti-GSK3β (glycogen synthase kinase-3 β) antibody, anti-APP antibody and anti-Cyclin D1 antibody were purchased from Abcam (UK). Anti-Aβ 1–42 antibody (Abcam UK, ab201060) for western blotting could detect both monomer (4 kDa) and high molecular weight oligomer (45 kDa), with the latter demonstrated in this study. Anti-Pin1 antibody were purchased from ProteinTech (USA). Anti-*cis* P-Tau antibody, anti-*trans* P-Tau antibody and anti-oxPin1 antibody were kindly provided by Professor Lu Kun Ping (Chen et al., 2015a). Anti-rabbit IgG alkaline phosphatase-linked secondary antibody was purchased from GE Healthcare (USA). Bicinchoninic acid (BCA) protein assay kit was purchased from Thermo Fisher Scientific (USA). Cell lysis buffer RIPA for western blots and Cell Counting Kit-8 were purchased from Phygene (China). Polyvinylidene difluoride (PVDF) membrane was purchased from Millipore Immobilon (USA). Chemiluminescence reagent mixture ECL Plus was purchased from Tanon (China). Loading buffer for western blot, DAPI and Goat

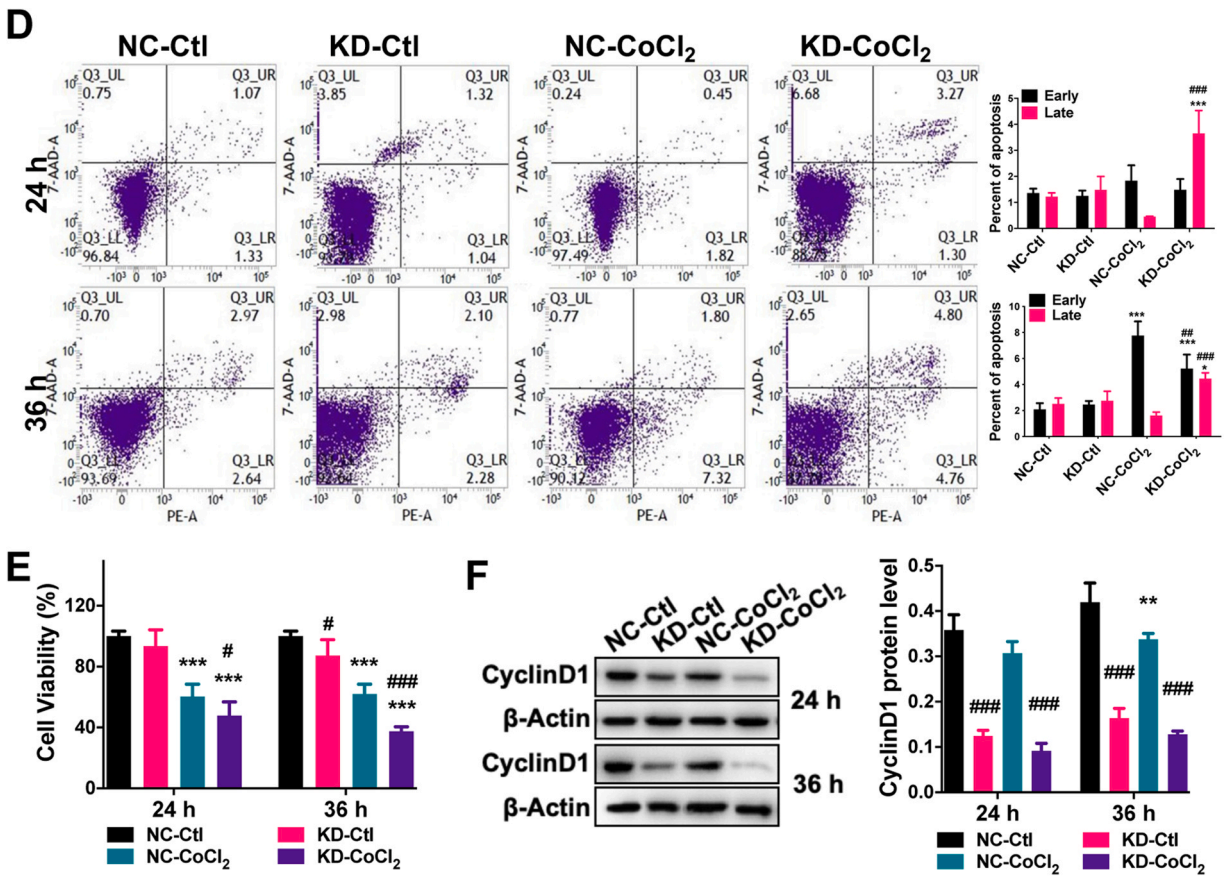

Fig. 2. (*continued*).

Anti-Mouse IgG/FITC were purchased from Solarbio (China). Horseradish peroxidase (HRP)-labeled goat anti-rabbit IgG (H + L) secondary antibody, Hoechst 33258 staining kit and Lipid Peroxidation MDA Assay Kit were purchased from Beyotime Biotechnology (China). Penicillin-Streptomycin Solution and Dulbecco's Modified Eagle Medium were purchased from Hyclone (USA). Fetal bovine serum was purchased from Gibco (USA). FITC/ Annexin V apoptosis detection kit and PI/RNase staining buffer were purchased from BD Biosciences Pharmingen (USA). Lentiviruses LV3-Pin1 and LV5-Pin1 were packed by GenePharma (China). Pin1 inhibitor all-trans retinoic acid (ATRA) and Juglone were purchased from Macklin (China) and Alfa Aesar (UK), individually. For blood samples from patients, K2-EDTA-coated tubes were purchased from BD Biosciences (USA) and the Lymphocyte Separation Medium from Hao Yang Biological Manufacture (China).

2.2. H4 cell culture and exposure

H4 human neuroglioma cells (H4 cells) are selected for higher relevance of H4 cells data's utility for the sequence of events leading to neurodegeneration and AD. H4 cells were purchased from cell bank of Chinese Academy of Sciences (China Center for Type Culture Collection, China) and cultured in DMEM with 10% FBS, penicillin (100 U/ml) and streptomycin (50 g/ml). All cells were maintained in a humidified incubator containing 5% CO_2 at 37 °C. The medium was replaced every 2 days. H4 cells with 80% confluency were exposed to $CoCl_2$, as a representative of environmental inorganic cobalt exposure as well as a better comparison with other studies (Catalani et al., 2012b; Léonard and Lauwerys, 1990; Muñoz-Sánchez and Chánez-Cárdenas, 2019). The concentrations of $CoCl_2$ used in this study were determined in CCK8 pilot experiments. $CoCl_2$ exposure for 24 h at 100, 200, 400 and 600 μM caused cell damage in the range of 20–30% cell viability. The *in vitro* concentrations we used here (100–600 μM, 5.89–35.34 mg/L) has been wildly used for previous studies (100–500 μM, 20–50 mg/L) (Zheng et al., 2019; Gupta et al., 2020; Maliha et al., 2019; Olivieri et al., 2001b; Guan et al., 2015). For Pin1 overexpression, lentivirus LV5-Pin1 was transfected to H4 cells according to manufacturer's instructions. For Pin1 knockdown, lentivirus LV3-Pin1, pKLO plasmid and inhibitors ATRA and Juglone were used following the manufacturer's instructions.

2.3. Western blot

Briefly, tissue and cell lysates were extracted with RIPA buffer. Protein concentration was measured by BCA Protein Assay Kit. Protein samples were heated for 10 min at 100 °C in 1 × loading buffer. 20 μg proteins were separated by electrophoresis on a 10–15% Tris-glycine acrylamide gel and transferred to a PVDF membrane using Trans-Blot Cell (Bio-Rad, USA). The membrane was blocked with 5% of fat-free milk for 1 h at room temperature and then incubated with the needed primary antibody overnight at 4 °C. After washed with 1 × TBS containing 0.1% Tween 20 (TBST), the membrane was incubated with secondary antibody at room temperature for 1 h. After washed with TBST, the membrane was incubated in ECL reagents, and images were taken with the Tanon 5200 imaging system (Shanghai, China). The blots were analyzed with Image J software (USA) for band densities. For detecting oxidized Cys-113 of Pin1 (oxPin1), standard protocol was carried out as described in (Chen et al., 2015b). Briefly, the membranes were blocked with 3% bovine serum albumin (BSA) in PBST for 1 h at room temperature, followed by incubation with anti-Oxy-Cys113 polyclonal antibody (1:1000) for 2 h at room temperature. Following the primary antibody incubation, the membranes were washed three times in Wash Blot for 5 min each and incubated with ECL Plex Cy5 Dye conjugated anti-rabbit antibody for 1 h in dark at room temperature. The

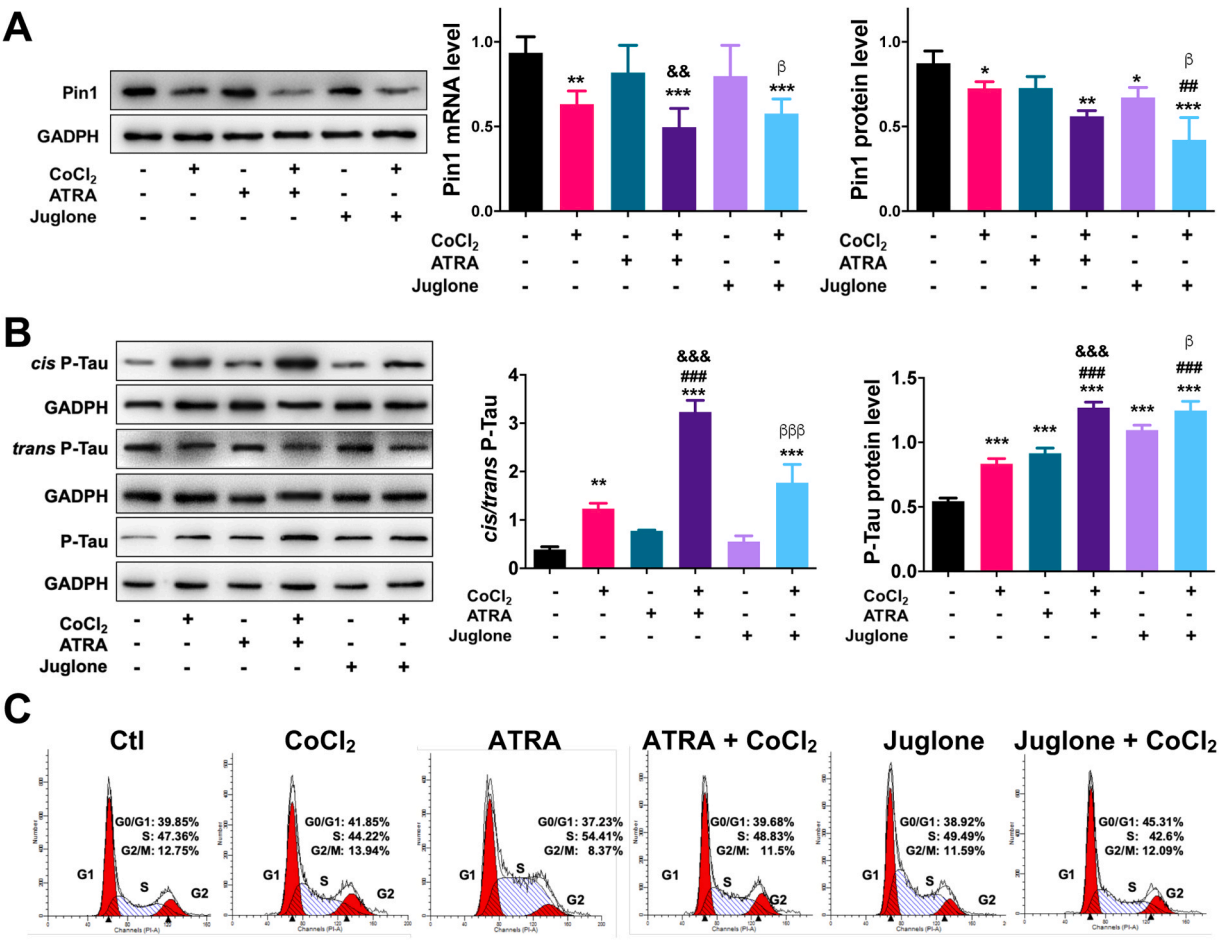

Fig. 3. Effects of cobalt on neurotoxicity in H4 cells with Pin1 knockdown. In order to explore the functional role of Pin1, its inhibitors ATRA and Juglone were evaluated in cells exposed to 200 μM $CoCl_2$ for 72 h. (A) Pin1 protein levels were downregulated by Pin1 inhibitors, and cobalt exposure induced further decrease in Pin1 protein levels. (B) The ratio of *cis/trans* P-Tau and P-Tau protein levels were further increased upon Pin1 inhibition. (C) Cell cycle arrest caused by cobalt exposure, with quantification presented in (D). (E) CyclinD1 protein level further decreased upon cobalt exposure in respective ATRA and Juglone groups (Pin1 inhibitor +/- cobalt groups), which corresponds with cell cycle arrest. (F) Apoptosis rates increased upon $CoCl_2$ exposure detected by Hoechst staining and Annexin V/ PI-flow cytometry. (G) Quantification of apoptosis. (H) Absent cobalt exposure, H4 cells showed indistinguishable differences in cell viability, while in response to cobalt exposure, cell proliferation was more severely impaired by cobalt in the presence of ATRA and Juglone, compared with WT + $CoCl_2$ group. Data analyzed with the CCK8 assay are shown as mean ± SD (n = 6). *$P < 0.05$, **$P < 0.01$ and ***$P < 0.001$ compared with WT H4 cells without Pin1 inhibitor neither cobalt exposure; # $P < 0.05$, ## $P < 0.01$ and ### $P < 0.001$ compared with WT H4 cells upon cobalt exposure; & $P < 0.05$, && $P < 0.01$ and &&& $P < 0.001$ compared with ATRA exposed H4 cells; β for $P < 0.05$, ββ< 0.01 and βββ $P < 0.001$ compared with Juglone exposed H4 cells. Scale bar, 500 μm.

membranes were washed in Wash Blot three times for 5 min each and the membrane was scanned with the Storm860 PhosphoImager (GE Healthcare). The densities of protein bands were measured using ImageJ software. The relative expression levels of target proteins were quantified with those of housekeeping proteins. Then, the expression levels were statistically analyzed.

2.4. Cell cycle and apoptosis measurement

H4 cells at log phase were collected and seeded to 60 mm plates at a cell density of 2×10^5 cells/ml. Cells were exposed to $CoCl_2$ in triplicates as noted above. After fixation, cells were dyed with PI staining buffer. Cell cycle was then detected by flow cytometry (BD FACSVerse) with the excitation of 488 nm. For apoptosis measurement, the same procedure was performed, followed by FITC/ Annexin-V apoptosis kit and flow cytometry detection (488/530 nm). Apoptosis was also measured with the Hoechst 33258 staining kit. Four fields were taken in each well by inverted fluorescence microscope (Olympus, Japan). The fluorescence was measured at 350 nm/ 460 nm (excitation/emission) wavelengths under Leica DMi8 fluorescence microscope. The intensity of fluorescence was measured by ImageJ.

2.5. Quantitative real-time PCR

Total cellular RNA was isolated using TRIzol reagent according to the manufacturer's instructions. cDNA was prepared using the PrimeScript® 1st Strand cDNA Synthesis Kit and assessed by quantitative real-time reverse transcription polymerase chain reaction (RT-PCR) using LightCycler 480 Real-Time PCR System (Roche, Switzerland). An aliquot of each PCR-amplified product was resolved *via* agarose gel electrophoresis, stained with ethidium bromide and photographed under ultraviolet light. For the respective samples, the PCR product values were normalized to the GAPDH PCR product values. The primer sequences selected from the detected gene for cDNA amplification are listed. Pin1 forward: 5'-TGATCAACGGCTACTACCAG-3' and reverse: 5'-CAAACGAGGCGTCTTCAAAT-3'. Gapdh forward: 5'-GGCACAGTCAAGGCTGAGAATG-3' and reverse: 5'-ATGGTGG TGAAGACGCCAGTA-3'.

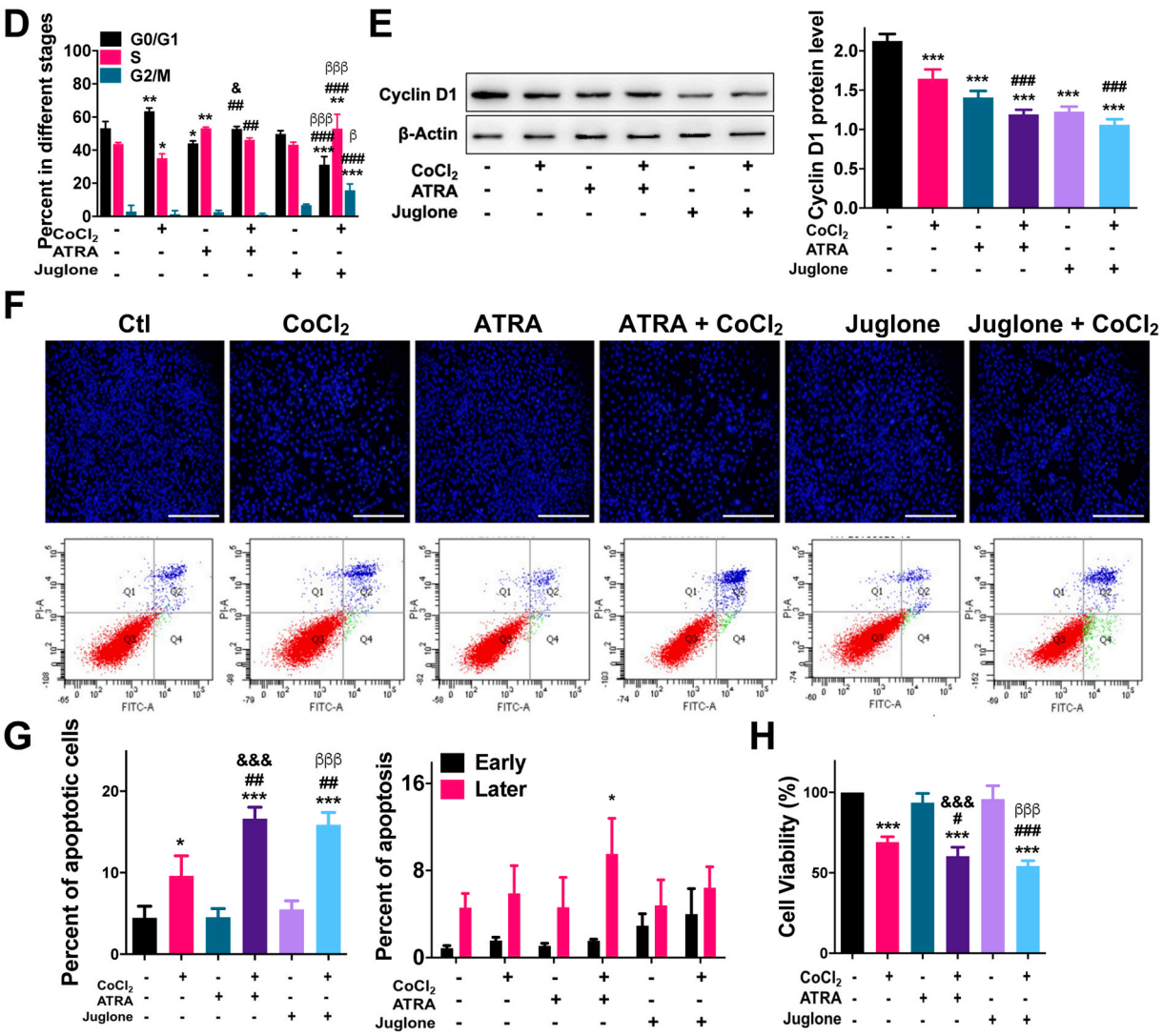

Fig. 3. (*continued*).

2.6. Animals and exposure

Male C57BL/6J mice were used in this study. The mice aged 8 weeks (15–26 g) and 48 weeks (24–39 g) were used to determine $CoCl_2$ toxicity and the effect of Pin1 in different age range. Mice were randomly allocated into 4 groups: 0 (saline), 4, 8 and 16 mg/kg of $CoCl_2$ groups. Next, mice from each group were intraperitoneal injected once a day for 30 days. All animal experiments were performed with proper care in accordance to the Guide for the Care and Use of Laboratory Animals. Animals were housed in the barrier environment of animal experiment center of Fujian Medical University with relative humidity at 60 ± 10%, room temperature of 20 ± 2 ℃ and a 12 h of light/dark cycle. The C57BL/6J mice were fed with standard laboratory chow. Food and water were provided ad libitum. All animals were kept in stress-free, hygienic and animal-friendly conditions.

According to ICP-MS results *in vivo*, the blood cobalt level in mice was 1.5969, 2.7265 and 3.4584 μg/l in three exposure groups (4, 8, and 16 mg/kg), respectively. These doses are clinically relevant in MoM hip replacement patients according to blood cobalt levels detected by ICP-MS. The hip replacement patients have an endogenous blood cobalt level of 2.514 μg/l (median). Therefore, our mice exposure doses are comparable with endogenous cobalt exposure patients.

2.7. Inductively coupled plasma mass spectrometry (ICP–MS)

Mice experiments were carried out as previously described (Zheng et al., 2019). For blood samples from humans, 200 μl of plasma was digested in 8 ml of nitric acid (69.5% v/v) for 40 min, followed by 2 h in 115 ℃ to remove acid. The samples were diluted with 1% nitric acid to final volume of 15 ml, followed by an analogous detection procedure. Values lower than the detection limit were set to the limit as 0.060 μg/l.

2.8. HE staining, silver impregnation and nissl staining

Brains of mice were fixed with 4% paraformaldehyde and transferred to 70% of ethanol. Next, the brains were placed in processing cassettes, dehydrated through a serial of alcohol gradients, and embedded in paraffin wax. Then, 5-μm-thick brain tissue sections were dewaxed in xylene, rehydrated through decreasing concentrations of ethanol, and washed in running water. Tissues were stained with haematoxylin and eosin, silver nitrate and silver ammonia solution, or toluidine blue.

2.9. TUNEL assay

To label apoptotic nuclei, the 3'-OH end of DNA fragments were visualized by the method of terminal transferase-mediated dUTP nick end-labeling (TUNEL). The TUNEL assay was performed according to

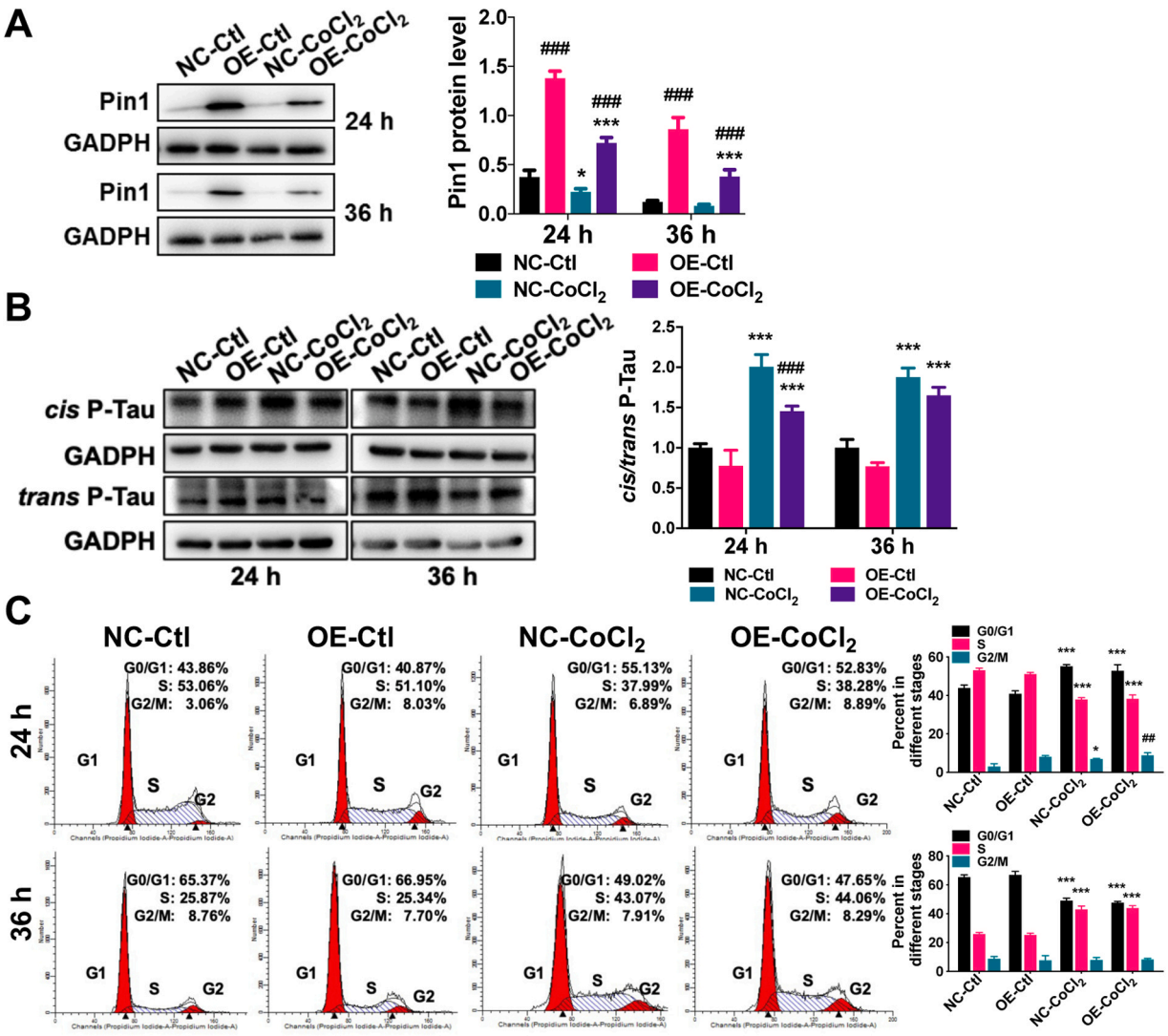

Fig. 4. Effects of cobalt on neurotoxicity in H4 cells with Pin1 overexpression. Pin1 overexpressing cells (labeled as OE) were exposed to 400 μM $CoCl_2$ for 24 h or 36 h. (A) Pin1 was upregulated by lentivirus overexpression vector. Cobalt exposure induced a reduction of Pin1 protein levels. (B) Protein expression of *cis* and *trans* P-Tau in response to $CoCl_2$ is shown. The ratio of *cis/trans* P-Tau protein level was presented next to the western blot. (C) $CoCl_2$ caused cell cycle arrest in G0/G1 phase after 24 h exposure and in S phase after 36 h exposure. (D) Apoptosis rates increased upon $CoCl_2$ exposure as detected by Annexin V/ PI-flow cytometry. (E) Absent cobalt exposure, Pin1 H4 OE cells showed indistinguishable cell viability compared to WT cells. However, upon cobalt exposure, Pin1 OE rescued cell viability. Data represent mean ± SD (n = 6). (F) Cell cycle related protein Cyclin D1 was downregulated in H4 OE cells after 24 h and 36 h of $CoCl_2$ exposure. NC groups represented H4 cells transfected with control lentivirus, as a negative control (NC) of the Pin1 overexpression (OE) cells. $^{*}P < 0.05$, $^{**}P < 0.01$ and $^{***}P < 0.001$ when comparing groups on the presence and absence of cobalt exposure under the same Pin1 condition (within NC groups or within OE groups); # $P < 0.05$, ## $P < 0.01$ and ### $P < 0.001$ when comparing NC and *P*in1 OE cells under the same exposure conditions (in the presence or absence of cobalt).

the manufacturer's instructions. The nuclei of apoptotic and non-apoptotic cells were counterstained with DAPI (1 μg/ml). The labeled cells were analyzed by Leica DM3000 fluorescence microscope. The intensity of fluorescence was measured by ImageJ.

2.10. Immunostaining

H4 cells were fixed in 4% PFA/sucrose in PBS for 20 min at room temperature, quenched with 50 mM NH_4Cl in PBS for 10 min at room temperature (RT), and permeabilized with 0.2% Triton X-100 in PBS for 5 min at RT. Blocking was performed with 5% BSA for 30 min. Primary antibodies were diluted in 5% BSA and incubated at RT for 2 h, followed by PBS washes and incubation with corresponding secondary antibodies for 1 h at RT in the dark, with gentle mixing. Nuclei were stained with Hoechst. Fluorescence microscopy was performed on a Zeiss Axioskop 2 microscope and Axiovison software (Zeiss, v4.8). The intensity of fluorescence was measured by ImageJ.

2.11. Spatial learning

Mice were trained for 5 days in a 150 cm circular Morris water maze pool. The pool was filled to a depth of 25 cm with water that was maintained at 26 ℃. Milk was added to make water opaque (Liou et al., 2002a) where a 15 cm round platform was submerged in a fixed position 1 cm below water level and placed in the carter of one of the quadrants. Daily training session consisted of 4 trials (15–30 min intervals) starting from 4 randomized starting positions. Mice that failed to locate the platform within 1 min, were gently guided to the platform and left there for 10 s. Escape latency for each group was calculated using the average time of four quadrant tests on training days. Probe trials were conducted

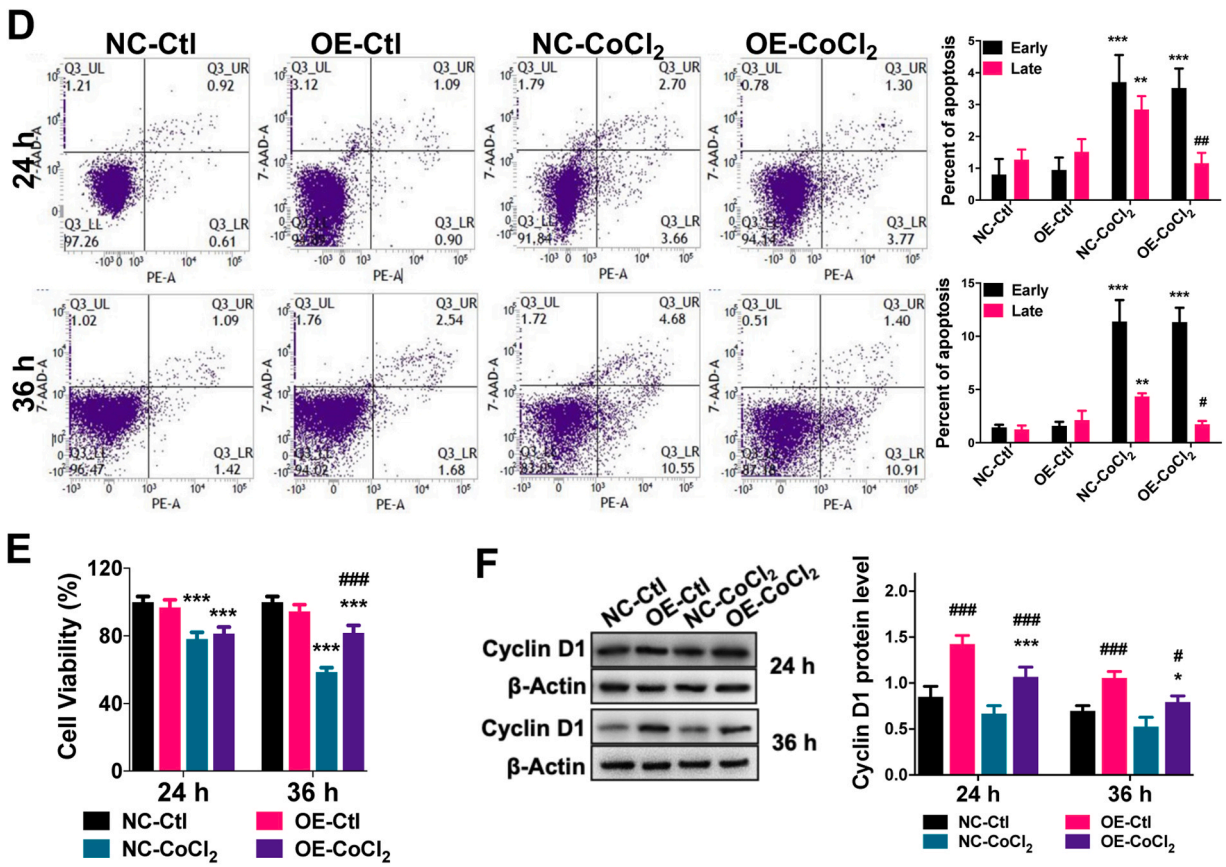

Fig. 4. (*continued*).

on day 6 after the 5-day training period, where the platform was removed from the pool and mice swam freely for 60 s. Mice were tracked with tracking equipment and software (Mobile Datum, China), which was used to calculate escape latency, path length and swimming velocity during training, and, during the probe trial, time spent in each quadrant and latency to first enter the target quadrant and target position.

2.12. Study population

In order to examine the clinical significance, we recruited hip replacement patients. 30 questionnaires, including 16 cases and 14 controls, were distributed, and all were collected from Department of Orthopaedics, Fuzhou Second Hospital between July 2019 and October 2019, China. Each patient underwent primary MoM total hip arthroplasty at an average of 6 (3–15) years before revision. For the inclusion in the study, cobalt exposure group was defined using the following criteria: (1) patients were required to have had a MoM hip prosthesis and at least one year after surgery, without proven infection or fracture; (2) patients are between 45 and 65 years old; (3) patients had no other metal prosthesis in the body; (4) patients had no functional abnormality in liver or kidney. Subjects without hip replacement during the same period were selected as controls. The control group had no working experience in metal factories, neither lived near the factories. All subjects were long-term residents in Fujian. Subjects who were taking drugs containing cobalt, chromium, or have failed to provide complete clinical data or with poor adherence were excluded from the study.

2.13. Questionnaire survey

All interviewers were specially trained before conducting the standard questionnaire. The questionnaire included demographic characteristics (age, gender) as well as clinical physiological and biochemical indicators (red blood cells, glucose, total cholesterol, high-density lipoprotein, low-density lipoprotein, *etc.*).

2.14. Blood samples

Blood samples were collected in a K2-EDTA-coated tube and centrifuged at 3500 *g* for 10 min, 4 °C to separate plasma. Following the manufacturer's instructions for the lymphocytes' separation medium, blood samples were further processed to obtain leukocytes and then the samples were stored at −80 °C. Plasma was used for the determination of cobalt concentration and peripheral blood leukocytes were used for WB detection.

2.15. Statistical analysis

The results were analyzed using the SPSS version 19.0. For the water maze experiment, the latency was analyzed by multivariate analysis of variance (ANOVA) of repeated measurement data. For space the probe trials, speed before entering the platform was analyzed by the rank sum test. The rests were analyzed by one-way ANOVA. For comparison among multiple groups, the least significant difference (LSD) *post-hoc* test was used. For plasma cobalt levels, nonparametric tests were applied. For blood protein levels, student *t*-test was applied. A P value <0.05 was considered statistically significant in all cases.

2.16. Ethics approval

All procedures performed in studies involving human participants were in accordance with the ethical standards of the institutional and/or national research committee and with the 1964 Helsinki declaration and its later amendments or comparable ethical standards. The protocol was approved by the ethics committee of Fuzhou Second Hospital (Sheet No.

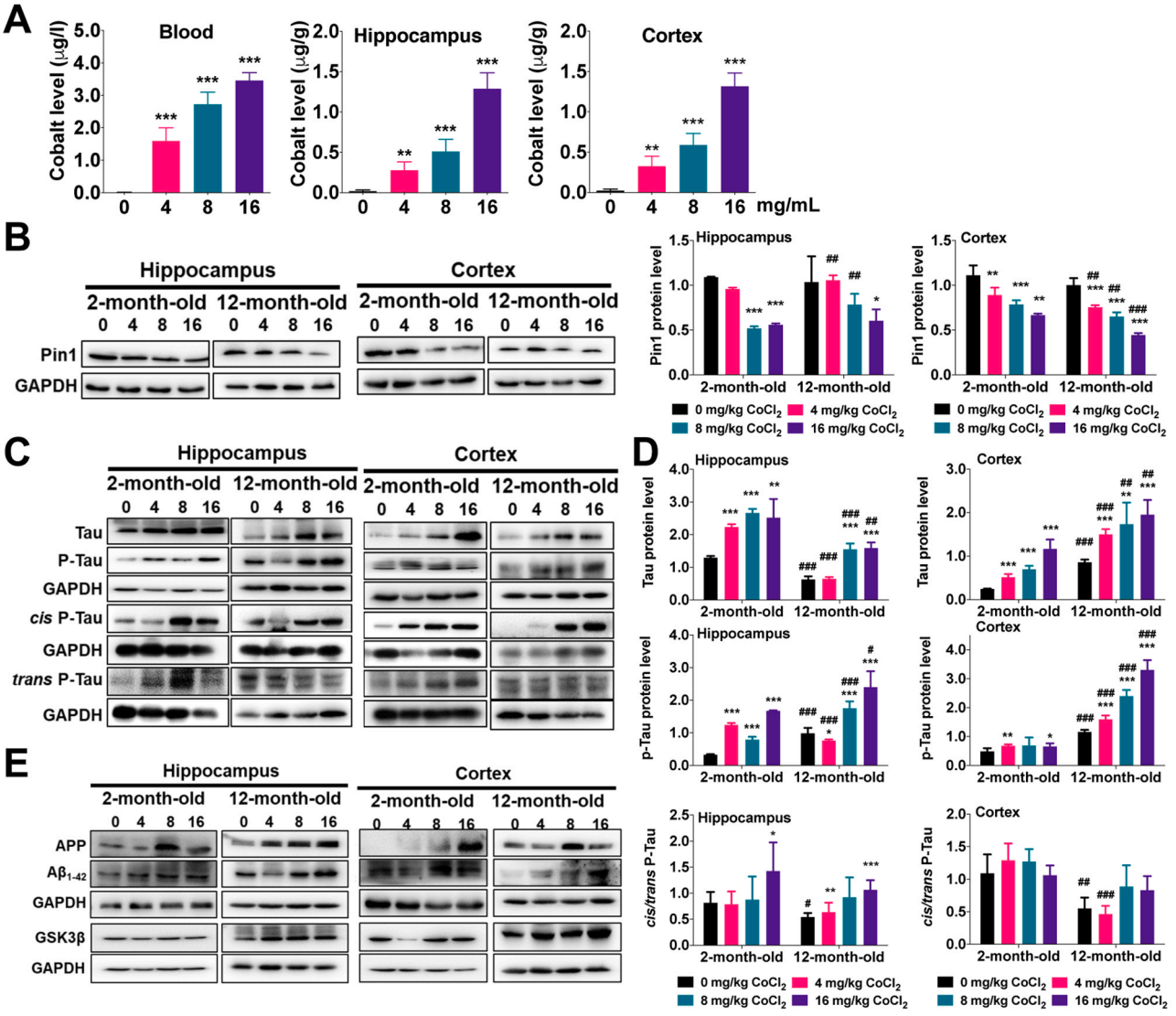

Fig. 5. Neurodegenerative effects of cobalt in 2- and 12-month-old mice. (A) After exposure, Co^{2+} content increased in the blood, cortex, hippocampus of 12-month-old mice (n = 5). (B) Protein levels of Pin1 in the hippocampus and cortex were significantly downregulated by cobalt regardless of age. (C) The upregulation of Tau, T231 P-Tau protein levels as well as *cis-/trans-* P-Tau ratio by cobalt marks the involvement of Pin1 in the process. (D) Quantification of (C). (E) The upregulation of APP, $A\beta_{1-42}$ and GSK3β marks the neurodegeneration caused by cobalt. (F) quantification of (E). (G) Neuronal apoptosis detected by TUNEL assay in both the hippocampus and cortex of 12-month-old mice. Scale bars of the upper panels indicate 100 μm, while in the zoom-in images, the scale bars indicate 50 μm. (H) Cobalt caused upregulations of apoptosis relative protein Caspase-9 in both the hippocampus and cortex from 2- and 12-month-old mice. (I) Results of histopathological examination in both the hippocampal and cortex of 12-month-old mice (n = 3) are shown. Left panel: HE staining with pyknosis of neuron indicated as red arrow, while red nerve cell labeled as yellow arrow. Middle panel: Bielschowsky's silver staining with fiber tangles and age spots marked with black arrow. Right panel: Nissl staining with Nissl's body noticed with black arrow. Scale bar indicates 500 μm. (J–N) Morris water-maze test showed learning and recognition deficiencies were caused by cobalt exposure (n = 5). In training trials (J), the representative tracks for each group were shown. In 2-month-old mice, all exposure group presented significant differences in all days. In 12-month-old mice, escape latencies in 8 and 16 mg/kg groups are significantly longer than the control group of the same day, as well as day 2 and day 4 of 4 mg/kg groups ($P < 0.05$). Space prob trials results including representative tracks (K), number of virtual platform crossings (L), swimming speed (M, cm/s) and time spent (N) in the effective region (seconds) of the mice are presented. All data are shown as mean ± SD. * for $P < 0.05$, ** $P < 0.01$ and *** $P < 0.001$ compared with the control in respective age group; # for $P < 0.05$, ## $P < 0.01$ and ### $P < 0.001$ compared with relative 2-month-old mice. (For interpretation of the references to colour in this figure legend, the reader is referred to the web version of this article.)

2019-2-1). All selected patients and controls provided informed consent. All applicable institutional and/or national guidelines for the care and use of animals were followed.

3. Results

3.1. Effects of cobalt on Pin1 and neurotoxicity in H4 cells

We examined the effects of paraquat, manganese, cobalt and aluminum on Pin1 protein expression on human neuroglioma (H4) cells after 36 h exposure (Fig. S1). Only cobalt induced Pin1 downregulation in a concentration-dependent manner (Fig. 1A). Furthermore, cobalt especially at high doses (400 and 600 μM) also induced Pin1 oxidization on the active site Cys113, (oxPin1), which also suggested the inactivation of Pin1 activity and its function in AD (Fig. 1A, B). To further determine the effects of cobalt on Pin1 isomerase activity in neurons, we assayed protein levels of T231 phosphorylated Tau (P-Tau) as well as its *cis* and *trans* isoforms because Pin1 catalyzes *cis* to *trans* isomerization of

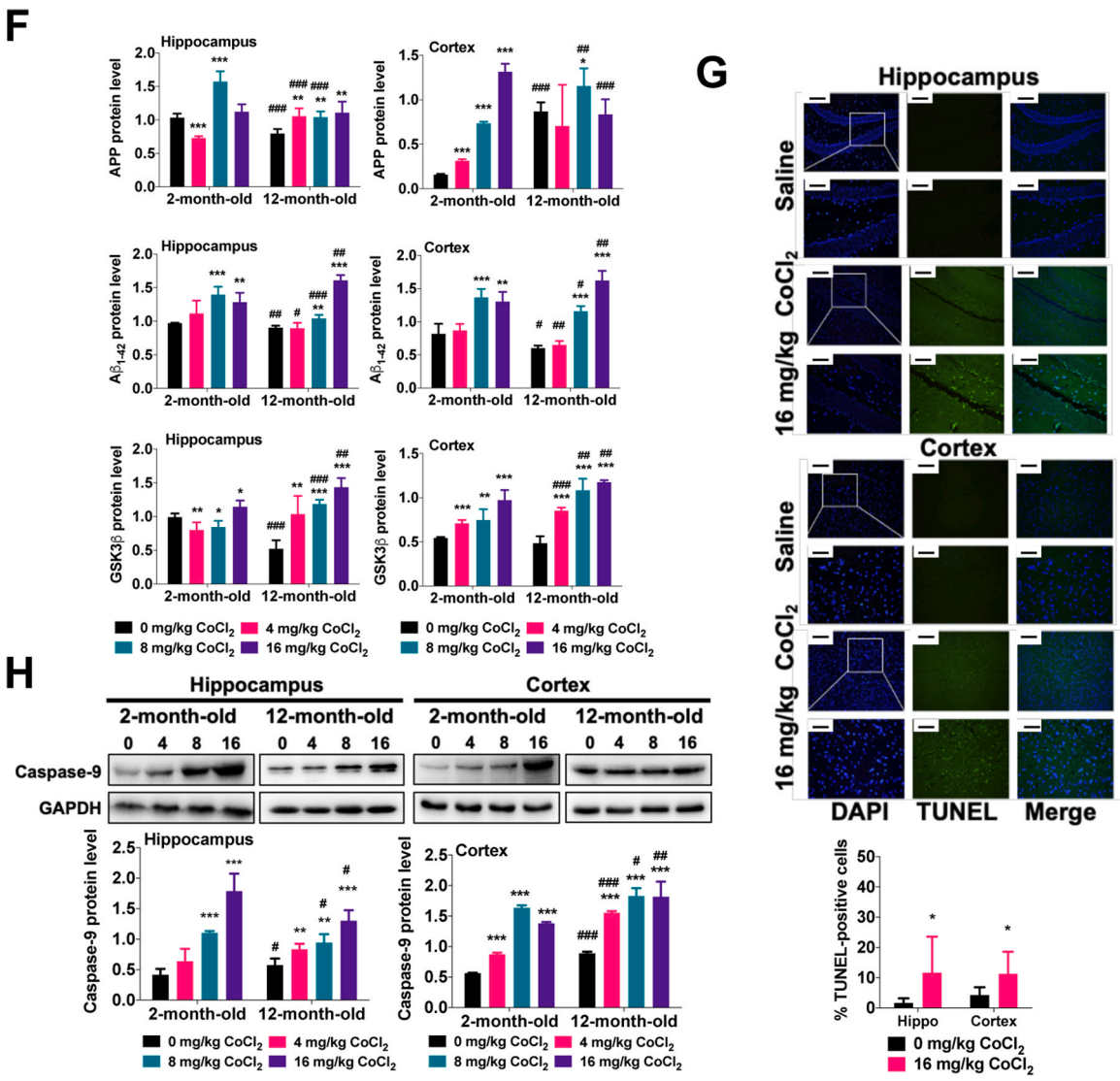

Fig. 5. (*continued*).

P-Tau. Indeed, cobalt increased the ratio of *cis/trans* P-Tau after 24 h and 36 h exposure in a concentration-dependent manner (Fig. 1C). These results were accompanied by concentration-dependent increases in total T231 P-Tau (Fig. 1C) as expected because unlike *trans*, *cis* P-tau is more resistant to protein dephosphorylation and degradation (Nakamura et al., 2012).

Since *cis* P-tau induces apoptosis in neurons (Kondo et al., 2015), we then assayed the effects of cobalt on the cell cycle and apoptotic profiles using FACS analyses. Cobalt concentration- and time-dependently induced cell cycle arrest in the G0/G1 stage Fig. 1D) and cell apoptosis (Fig. 1E, F). Late apoptotic cells, as detected by Annexin V/PI-flow cytometry and defined as Annexin$^+$/PI$^-$, increased in both the 24 and 36 h cobalt exposure groups, while early apoptosis (defined as Annexin$^+$/PI$^+$) was significantly upregulated only after 36 h exposure (Fig. 1F). The above cell cycle and apoptotic phenotypes were further supported by reduced protein levels of Cyclin D1, whose activity is required for cell cycle G1/S transition (Massagué, 2004) and whose protein levels are upregulated by Pin1 (Liou et al., 2002b), and increased protein levels of Caspase-9 (Fig. 1G), which is critical for apoptosis (Bratton and Salvesen, 2010).

3.2. Effects of cobalt on neurotoxicity in H4 cells with Pin1 inhibition

To further support that cobalt-induced Pin1 downregulation is critical for cobalt to induce the above neurotoxicity phenotypes, we used Pin1 genetical knockdown or chemical inhibition to examine whether either or both would aggravate cobalt neurotoxicity. For Pin1 knockdown, we generated Pin1 knockdown (KD) stable cells using the validated shPin1 lentivirus (Nakamura et al., 2012). Pin1 was significantly downregulated to 28.5% and 22.7% of control (24 and 36 h) in Pin1 KD cells (Fig. 2A). In addition, the *cis/trans* P-Tau ratio was further upregulated upon cobalt exposure in Pin1 KD cells in 36 h. T231 P-Tau protein level was upregulated by Pin1 KD. When comparing KD-Ctl and KD-$CoCl_2$ cells, downregulation of P-Tau was observed in response to cobalt exposure (Fig. 2B). Cell cycle arrest in the G0/G1 stage was noted after 24 h of cobalt exposure in Pin1 KD cells, whereas after 36 h exposure, cell cycle was arrested in the S stage (Fig. 2C). Apoptotic cells increased in Pin1 KD cells upon cobalt exposure (Fig. 2D). Correspondingly, the reduction in cell viability upon cobalt exposure was more pronounced in KD-$CoCl_2$ than NC-$CoCl_2$ cells, with 20.95% (24 h) and 39.34% (36 h) downregulation, respectively (Fig. 2E). Combined with Fig. 2A's result, the cobalt exposure accounted for 40.5% decrease, while Pin1-KD was obligated to a further 12.7% decrease in 24 h. Similarly, Pin1-KD accounted for 24.4% in 48 h treatment.

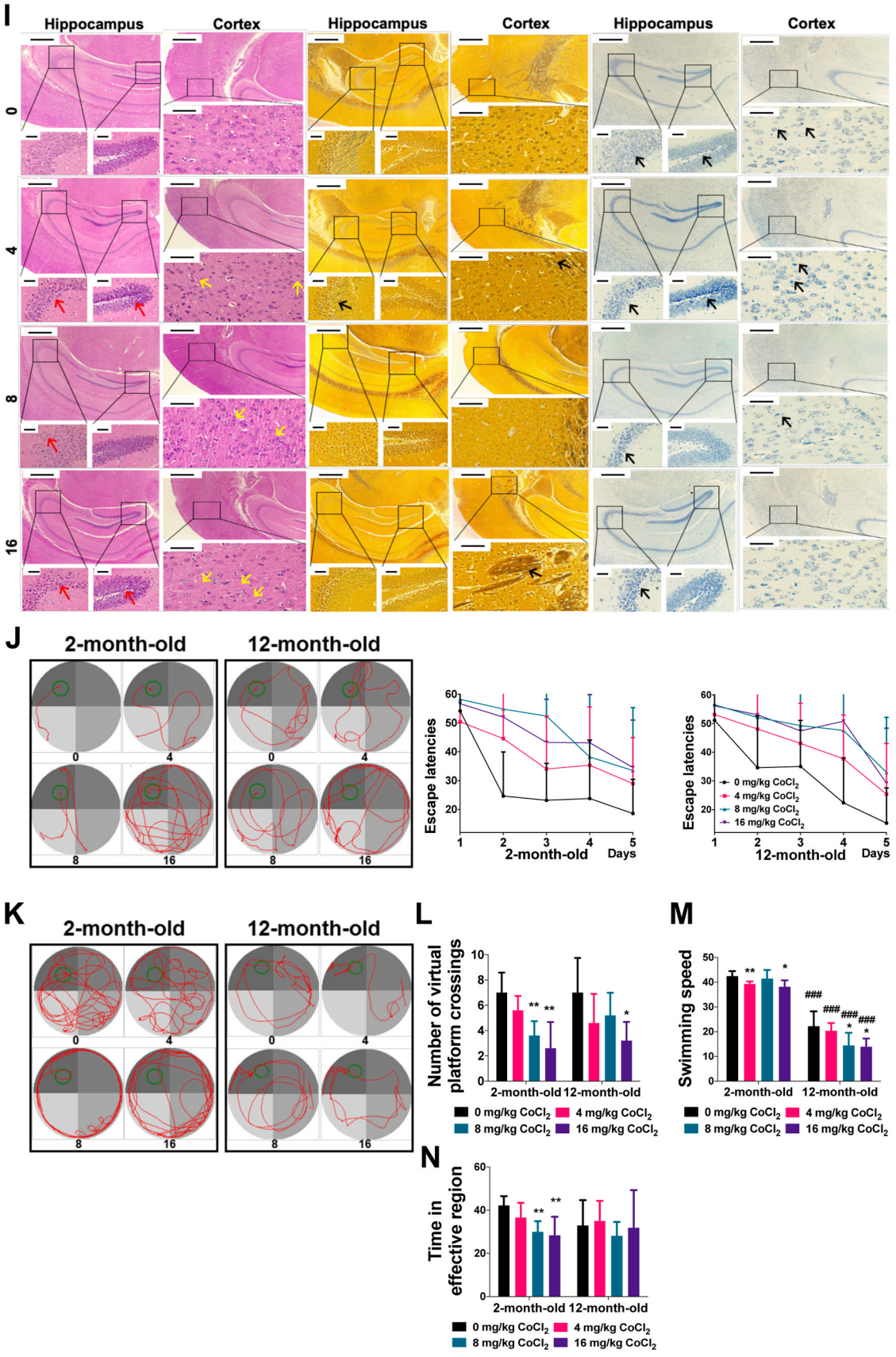

Fig. 5. (*continued*).

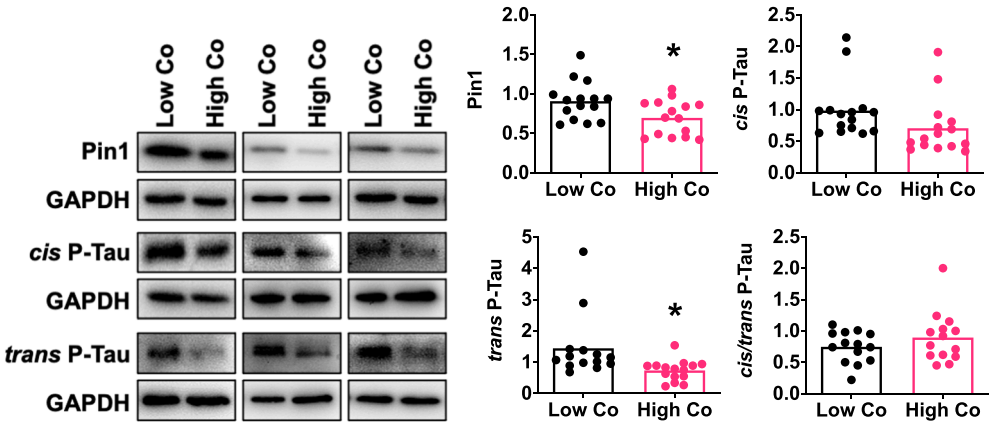

Fig. 6. Examinations of Pin1 protein level and function in human blood samples from hip joint replacement. Human sample data were divided into low Co (low cobalt) and high Co (high cobalt) groups according to the median plasma cobalt level (0.669 μg/l). Blood cell Pin1 and *trans* P-Tau protein levels were significantly decreased in the high cobalt group. * for $P < 0.05$ compared with the control.

Table 1
Cobalt, Pin1 and P-Tau levels in hip joint replacement patients.

Indices	Low Co (n = 15)	High Co (n = 15)	Z or *t*	*P*
Cobalt level	0.060 (0.060, 0.060)	2.514 (1.701, 6.831)	-4.822	<0.001*
Pin1	0.908 ± 0.245	0.696 ± 0.221	2.488	0.019*
cis P-Tau	0.984 ± 0.451	0.706 ± 0.443	1.703	0.100
trans P-Tau	1.444 ± 1.033	0.736 ± 0.331	2.523	0.018*
cis/trans P-Tau ratio	0.747 ± 0.252	0.895 ± 0.405	-1.162	0.256

Cobalt level presented as P50 (P25, P75) format in percentiles. In the low cobalt group, samples falling under the detection limit were set to the same value of detection limit (0.060). Pin1, cis P-Tau, trans P-Tau protein levels and the ratio are shown as mean ± SD. * for $P < 0.05$ determined with either nonparametric tests or independent student *t*-test.

Corroborating the results in Fig. 1, Cyclin D1 was downregulated in response to cobalt exposure. The decrease in Cyclin D1 protein level in Pin1 KD cells was consistent with cell cycle arrest (Fig. 2F).

For Pin1 inhibitors, we tested two Pin1 inhibitors ATRA and Juglone (Wei et al., 2015; Wang et al., 2017). In order to fully inhibit the Pin1 levels, the exposure was extended to 72 h, while the concentration was decreased to 200 μM, as the CCK8 result demonstrated a similar defect of 400 μM, 48 h. Juglone reduced Pin1 protein but not mRNA level, while ATRA did not decrease both in mRNA and protein of Pin1. Cobalt exposure led to a decrease in Pin1 mRNA and a further reduction in protein levels upon Pin1 inhibition by Juglone. Instead, ATRA inhibition in combination with cobalt exposure only resulted in mRNA reduction (Fig. 3A). Moreover, the *cis/trans* P-Tau ratio was upregulated after cobalt exposure in all three exposure groups. Similarly, T231 P-Tau protein levels were upregulated by Pin1 inhibitors in the absence of cobalt. This upregulation of P-Tau protein was more prominent upon cobalt exposure (within Pin1 inhibitor groups). It is noteworthy, the Pin1 inhibitors-induced increase in P-Tau and *cis/trans* P-Tau ratio was further increased by cobalt, possibly by reduction of residual Pin1 expression (Fig. 3B). The cell cycle was arrested in Pin1 inhibitor groups, with further reduction observed upon cobalt (Fig. 3C, D). A decrease in CyclinD1 was found in the presence of both inhibitors, and further reduction was observed in response to cobalt exposure (Fig. 3E). Greater number of apoptotic cells was found by both Hoechst staining and Annexin V/PI staining in cobalt-exposed cells in the presence of the Pin1 inhibitors and cobalt exposure (*vs.* cobalt exposure alone) (Fig. 3F, G). Corroborating the Pin1 KD results, aggravated cellular damage was noted in the presence of both cobalt and Pin1 inhibitors (Fig. 3H).

3.3. *Effects of cobalt on neurotoxicity in H4 cells with Pin1 overexpression*

To further confirm the causal relationship between cobalt and Pin1, we examined whether stable Pin1 overexpression (OE) would rescue

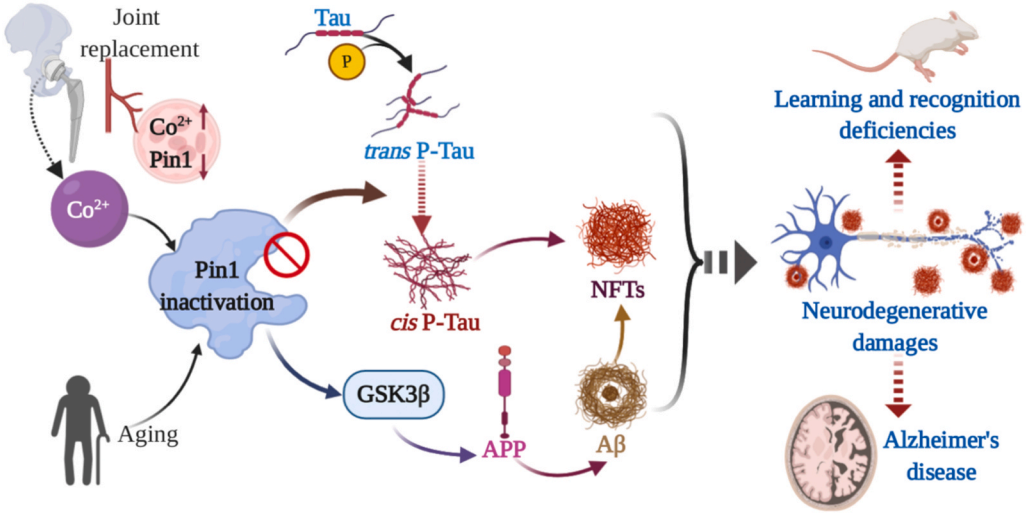

Fig. 7. Pin1, cobalt and aging mediate neurodegenerative damages. Here, we suggest that neurodegenerative damages are contributed by cobalt and aging. Cobalt exposure inactivates Pin1, on one hand, results in *trans* P-Tau to *cis* P-Tau transformation. On the other hand, Pin1 repression activates GSK3β, followed by amyloid precursor proteins (APP) and beta-amyloid (Aβ) generation. Both pathways lead to the formation of neurofibrillary tangles (NFTs). These alternations in molecular levels *in vitro* is in line with the neurodegenerative damages *in vivo:* learning and recognition deficiencies in mice models as well as joint replacement patients with excess cobalt containing less Pin1 proteins in human samples. Aging promotes P-Tau transformation and neurodegeneration in this context.

cobalt-induced neurotoxicity in H4 cells. Cobalt exposure led to decreased Pin1 protein levels (Fig. 4A). Corroboratively, after 24 and 36 h cobalt exposure, the increase of *cis/trans* ratio in Pin1 OE cells was increased to a lesser extent, suggesting the role of Pin1 (Fig. 4B). Cell cycle arrest in G0/G1 stage and S stage was found 24 h and 36 h after cobalt exposure in Pin1 OE cells, individually (Fig. 4C). Apoptosis was induced in Pin1 OE cells by cobalt, but were alleviated by Pin1 overexpression (Fig. 4D). Moreover, the cobalt-induced decrease in cell viability was partially rescued by Pin1 overexpression in 36 h (Fig. 4E). Finally, Cyclin D1 was indeed upregulated by Pin1 OE, supporting the cell cycle and viability results (Fig. 4F).

3.4. Effects of cobalt on Pin1 and neurodegenerative damages in mice

Here, we employed the *in vivo* model to investigate the role of cobalt and Pin1. Firstly, ICP-MS was performed to examine the distribution of cobalt ions in varying parts of brains, including blood, cortex and hippocampus. The levels of Co^{2+} in blood, cerebral cortex and hippocampus of cobalt-exposed groups were significantly higher than that of control group in a dose-dependent manner (Fig. 5A). In cobalt-exposed groups, disturbances of metal ions were also observed (Fig. S2). Consistent with the *in vitro* findings, we observed a dose-dependent decrease in Pin1 protein levels in the hippocampus and cortex of mice exposed to 8 or 16 mg/kg cobalt. When comparing 2- with 12-month-old mice, the reduction was more pronounced in the 12-month-old group (Fig. 5B). Pin1 isomerase activity was also inhibited in mice exposed to cobalt, as Tau, P-Tau and the *cis/trans* P-Tau ratio increased, especially at older age (Fig. 5 C & D for quantification). Previously, Pin1 reduction has been shown to activate GSK-3β, leading to phosphorylation and thus aggregation of APP and Tau (Pastorino et al., 2006; Nakamura et al., 2012). Therefore, we examined the effects of cobalt on the level of $A\beta_{1-42}$, APP and GSK3β. Upregulation of these proteins was observed in the hippocampus and cortex of both 2- and 12-month-old mice. In older mice, a dose-dependent increase in both $A\beta_{1-42}$ and GSK3β expression supports the notion that cobalt may trigger neurodegenerative damage in an age-dependent manner (Fig. 5E & F). Also, *in vivo* apoptosis was further strengthened by TUNEL assay (Fig. 5G). Corroborating the TUNEL findings and *in vitro* results, apoptosis in both 2- and 12-month--old mice was significantly increased by cobalt, as evidenced by the increase in Caspase-9 protein in both hippocampus and cortex (Fig. 5H). HE staining results indicated neuronal death caused by cobalt, which was manifested as neuronal pyknosis. In hippocampus and cortex, a significant increase in pyknosis of neuron and dark red neurons was seen in the exposure group compared with the control. Bielschowsky's silver staining revealed the increase of neuronal fiber tangles and age spots caused by cobalt. Furthermore, Nissl staining showed the reduction of Nissl's body caused by cobalt (Fig. 5I). To investigate potential cognitive deficits associated with cobalt exposure, Morris water-maze test was performed. Cognitive and memory weakening were found after cobalt exposure and advanced age. In training trials of the Morris water maze, mice treated with cobalt exhibited a longer escape latency and required more attempts to find the hidden platform in the water pool compared to control group, dose-dependently (Fig. 5J). A space probe trial was performed after the training trials by removal of the platform. The original platform location in the training trials was set as the virtual platform, number of crossings through the platform, time spent in the effective platform, as well as the paths in the virtual platform were recorded as neurobehavioral parameters (Fig. 5K). The swimming speed of 12-month-old mice group was slower than that of the 2-month-old group (Fig. 5M). The number of crossing the virtual platform and time spent in the effective region for the cobalt group was less than that of the control group (Fig. 5L & N).

3.5. Effects of cobalt on Pin1 in hip replacement patients

To examine whether cobalt exposure would affect Pin1 levels in human patients, we measured blood cobalt levels from patients underwent MoM hip prosthesis. Plasma cobalt levels in these patients (2.514 μg/l) were significantly higher than in the control group (0.06 μg/l). We then divided the human samples into low and high cobalt groups based on the median cobalt level (marked as Low Co and High Co groups). As demonstrated in (Table S1), baseline demographics of the two groups are statistically insignificant. We found that the high cobalt group had lower Pin1 protein levels as well as *trans* P-Tau levels (Fig. 6). Amongst the 30 samples tested, we failed to note statistical differences either for *cis* P-Tau protein level or *cis/trans* P-Tau ratio (Table 1).

4. Discussion

Cobalt is an established neurotoxicant (Tvermoes et al., 2015; Zheng et al., 2019, 2020; Guan et al., 2015). Moreover, we recently discovered that cobalt could cause neurodegenerative damages in mice (Guo et al., 2020; Tang et al., 2020b); whose mechanism(s) of toxicity have yet to be fully understood. In the present study, we show, for the first time, cobalt exposure results in Pin1 downregulation in the brain of 2- and 12-month-old mice as well as in human neuroglioma cells, indicating that environmentally toxicant-induced AD pathology might be mediated by changes in the expression and activity of Pin1, which was further confirmed in human patients (see Fig. 7 for mechanistic picture).

Previous studies on Pin1 have focused on its dual role in the context of cancer development (Pin1 activation) and AD (Pin1 inactivation) (Lanni et al., 2020; Sherzai et al., 2020). However, its role in neurodegenerative diseases induced by environmental toxicants has yet to be addressed. Amongst the environmental toxicants tested, Pin1 reduction upon exposures was only inherent to cobalt. We show here, upon Pin1 downregulation, cobalt caused cell damage, apoptosis and oxidative stress both *in vitro* and *in vivo*. Furthermore, cell cycle arrest and the decrease in its related protein Cyclin D1 were noted upon cobalt exposure. Moreover, consistent with our previous findings (Liou et al., 2002b), Cyclin D1 level was closely associated with Pin1 levels: when Pin1 was upregulated, Cyclin D1 increased, and vice versa. These data confirmed that cobalt induces apoptosis and cell cycle arrest through Pin1 inactivation.

The functions of Pin1 are regulated by various post-translational modifications, such as phosphorylation, oxidation, ubiquitination and SUMOylation (Chen et al., 2020b). Our findings show that mRNA and protein levels of Pin1 are both downregulated upon cobalt exposure, suggesting the possible mechanism of cobalt-induced Pin1 inactivation could be related to reduction in Pin1 mRNA and oxidative stress. An oxidative modification of Cys113 in the PPIase domain upon hydrogen peroxide could lead to Pin1 enzymatic activity abolishment (Chen et al., 2015a). Similarly, we demonstrate here oxPin1 upregulation and oxidative stress are induced by cobalt, suggesting that cobalt inactivates Pin1 through oxidation. Besides, there are several potential regulatory mechanisms worth exploration. For example, the insulin-resistant state reported in AD brain and the associated PI3K/Akt pathway correlate with Pin1 levels in patients (Liao et al., 2009; Barker et al., 2020). Further potential mechanism of cobalt inactivating Pin1 could be related to the energy regulating pathways (such as PI3K/Akt pathway), and molecules, *e.g.* mTORC1 (mammalian target of rapamycin 1) and cellular tumor antigen p53. Last but not least, the death-associated protein kinase 1 (DAPK1) (regulated by melatonin) decreases Ser71 phosphorylation of Pin1 (Chen et al., 2020a). Thus, additional investigations are encouraged to discover novel upstream regulators of Pin1.

Tau maintains the normal axonal microtubule network in neurons, and its phosphorylation is an early event in promoting tangle formation, which is inherent to AD (Lu et al., 2003). Pin1 binds to P-Tau and inhibits the development of Tau-mediated neurodegeneration by catalyzing the *cis* to *trans* conversion of P-Tau in AD (Lee et al., 2011). Our experiments suggest that as cobalt exposure increased, Tau and P-Tau

protein levels were upregulated, both *in vitro* and *in vivo*. Furthermore, both experimental platforms corroborated that the *cis/trans* P-Tau ratio was strongly and positively related to cobalt exposure, strengthening the relationship between cobalt and Pin1 inactivation in the context of neurodegeneration. In familial AD, abnormal APP processing leads to the formation of the Aβ peptide and aggregation (Hardy et al., 1998). Processing of APP can be regulated by phosphorylation, and proline-directed phosphorylation by GSK3β increases amyloid pathology (Lee et al., 2003). Moreover, Pin1 is necessary for APP's anchoring to the plasma membrane, favoring the non-amyloidogenic processing and reducing its internalization (Phiel et al., 2003). In this study, we have established the upregulation of GSK3β, APP and Aβ in response to cobalt, secondary to Pin1 inactivation. It would be plausible to expose cobalt to Pin1 overexpressed animals and check whether cobalt-induced toxicity was partially recovered. However, currently Pin1 *in vivo* overexpression is by the injection of Pin1 adenovirus, however, the protein expression would only last for 48 h (Risal et al., 2012). Moreover, as Pin1 shows dual role in Alzheimer's disease and cancers (Driver and Lu, 2010), it would be not applicable to overexpress Pin1 in long term (*i.e.* 30 days).

Clinically, in patients with hip replacement, cobalt levels were significantly elevated, possibly owing to an increased degree of wear and corrosion and with the occurrence of periprosthetic complications (*e.g.*, loosening) (Leyssens et al., 2017). Therefore, blood cobalt level has been proposed to monitor the conditions of prostheses in patients. However, the "safety threshold" of blood cobalt level in joint prostheses patients varies among different studies: a biokinetic model estimated 300 μg/l as safe (Paustenbach et al., 2013), while Sidaginamale et al. reported 4.5 μg/l as a threshold value for the detection of abnormal wear (Sidaginamale et al., 2013); over 20 μg/l was regarded as at risk for systemic toxicity by Van Der Straeten et al. (2013); another reported that for 10-year-exposure with a steady state of blood cobalt concentration of 10 μg/l is considered safe (Tvermoes et al., 2015). It is worth noting that in this study, the median blood cobalt level was lower than all the above (2.514 μg/l), accompanied with Pin1 reduction. The finding ascertained that cobalt caused Pin1 downregulation and potential neurodegenerative damages thereafter. Notably, in human AD patients, brain Pin1 expression levels were correlated with Tau tangles (Liou et al., 2002b). Our previous study has also demonstrated *cis* P-Tau accumulation in AD patients (Nakamura et al., 2012). Although we failed to observe significant changes in *cis* P-Tau nor *cis/trans* P-Tau ratio, a significant decrease in *trans* P-Tau was found in human samples containing high cobalt levels. One possible explanation might be that hip replacement patients recruited in this study were still at the early stages of neurodegenerative impairment, which very few markers were established (Dubois et al., 2016). Therefore, they failed to show alterations inherent to AD biomarkers (increase in *cis* P-Tau and *cis/trans* P Tau ratio). Cognitive impairment has been found in patients with hip joint replacement surgery (22%), known to progress AD (Wu et al., 2018). Therefore, the decrease of *trans* P-Tau can be an early detection biomarker of cognitive impairment in joint replacement patients processing to AD.

As the development of biological techniques, the antibodies against more biomarkers such as total Tau, Aβ and neurofilament light are available to test in human blood, serving as diagnosis evidence for AD and cognitive dysfunction (Blennow, 2017; Shaw et al., 2020). However, it is noteworthy Aβ levels in body fluids are subject to changes in AD and normal aging (Song et al., 2011; Herukka et al., 2017). Therefore, more investigations of *cis* P-Tau (Kondo et al., 2015) and other biomarkers in both blood and core cerebrospinal fluids are necessary in MoM hip replacement patients with larger sampling scales to further confirm this hypothesis. Besides, the concentration of potential biomarkers should be taken into account for easier detection in patients. Moreover, analyses of the characteristics of plasma exosomes (including morphology, number and pathological proteins) have been suggested to be of benefit in AD diagnosis, and it might therefore be applied to hip replacement patients for examination of AD risk (Sun et al., 2020; Hong et al., 2019).

In conclusion, we evaluated neurodegenerative changes in response to cobalt exposure, an environmental hazard. We have established that Pin1 plays a protective role by modulating GSK3β, APP, Aβ levels and shifting pathological *trans* P-Tau to physiological *cis* P-Tau. Aging is positively associated with the neurodegenerative sequalae of cobalt exposure and Pin1 inhibition. Our findings suggest that interaction among cobalt, Pin1 and aging promote neurodegeneration, and merit future studies on Pin1 as a putative therapeutic target in mitigating neurodegenerative processes associated with cobalt.

CRediT authorship contribution statement

Fuli Zheng: Conceptualization, Project administration, Writing - original draft, Writing - review & editing. **Yuqing Li:** Investigation, Writing - original draft. **Fengshun Zhang:** Investigation. **Yi Sun:** Software, Formal analysis. **Chunyan Zheng:** Methodology, Investigation. **Zhousong Luo:** Methodology, Investigation. **Yuan-Liang Wang:** Writing - review & editing. **Michael Aschner:** Visualization, Writing - review & editing. **Hong Zheng:** Resources. **Liqiong Lin:** Resources. **Ping Cai:** Methodology, Visualization. **Wenya Shao:** Visualization. **Zhenkun Guo:** Visualization. **Min Zheng:** Visualization. **Xiao Zhen Zhou:** Conceptualization, Visualization. **Kun Ping Lu:** Conceptualization, Visualization. **Siying Wu:** Supervision, Project administration. **Huangyuan Li:** Conceptualization, Supervision, Project administration, Visualization.

Declaration of Competing Interest

The authors declare the following financial interests/personal relationships which may be considered as potential competing interests: K. P.L. and X.Z.Z. are inventors of *cis* P-tau antibody technology, which was licensed by BIDMC to Pinteon Therapeutics. Both K.P.L. and X.Z.Z. own equity in Pinteon. Their interests were reviewed and are managed by BIDMC in accordance with its conflict-of-interest policy. Other authors declared that no competing interest exists.

Data availability

The authors declare that the main data supporting the findings of this study are within the article. Extra data are obtained from the corresponding authors upon request.

Acknowledgements

Funding: This work was supported by the Joint Funds for the innovation of Science and Technology; Fujian province [grant numbers 2017Y9105, 2019J05081], the National Natural Science Foundation of China [grant numbers 81973083, 81903352, 81601144]; and the Provincial Natural Science Foundation of Fujian Province [grant numbers 2017J01523, 2019J05081]. We would like to thank Junjin Lin, Zhihong Huang from the Public Technology Service Center (Fujian Medical University) for their technical assistance as well as Le Yang and Yeying Wen from the School of Public Health (Fujian Medical University) for coordinating and the handling the human subject specimens.

Appendix A. Supporting information

Supplementary data associated with this article can be found in the online version at doi:10.1016/j.jhazmat.2021.126378.

References

Barker, R.M., Holly, J.M.P., Biernacka, K.M., Allen-Birt, S.J., Perks, C.M., 2020. Mini review: opposing pathologies in cancer and Alzheimer's disease: does the PI3K/Akt pathway provide clues? Front Endocrinol. 11, 403. https://doi.org/10.3389/fendo.2020.00403.

Becker, E.B., Bonni, A., 2006. Pin1 mediates neural-specific activation of the mitochondrial apoptotic machinery. Neuron 49 (5), 655–662. https://doi.org/10.1016/j.neuron.2006.01.034.
Blennow, K., 2017. A review of fluid biomarkers for Alzheimer's disease: moving from CSF to blood. Neurol. Ther. 6 (1), 15–24. https://doi.org/10.1007/s40120-017-0073-9.
Bolognin, S., Messori, L., Zatta, P., 2009. Metal ion physiopathology in neurodegenerative disorders. Neuromol. Med. 11 (4), 223–238. https://doi.org/10.1007/s12017-009-8102-1.
Bozic, Kevin J., 2009. The epidemiology of bearing surface usage in total hip arthroplasty in the United States. J. Bone Jt. Surg. Am. 91 (7), 1614–1620.
Bratton, S.B., Salvesen, G.S., 2010. Regulation of the Apaf-1–caspase-9 apoptosome. J. Cell Sci. 123 (19), 3209–3214. https://doi.org/10.1242/jcs.073643.
Bumoko, G.M., Sadiki, N.H., Rwatambuga, A., Kayembe, K.P., Okitundu, D.L., Mumba Ngoyi, D., Muyembe, J.J., Banea, J.P., Boivin, M.J., Tshala-Katumbay, D., 2015. Lower serum levels of selenium, copper, and zinc are related to neuromotor impairments in children with konzo. J. Neurol. Sci. 349 (1–2), 149–153. https://doi.org/10.1016/j.jns.2015.01.007.
Catalani, S., Rizzetti, M., Padovani, A., Apostoli, P., 2012a. Neurotoxicity of cobalt. Hum. Exp. Toxicol. 31 (5), 421–437. https://doi.org/10.1177/0960327111414280.
Catalani, S., Rizzetti, M.C., Padovani, A., Apostoli, P., 2012b. Neurotoxicity of cobalt. Hum. Exp. Toxicol. 31 (5), 421–437. https://doi.org/10.1177/0960327111414280.
Chen, C.-H., Li, W., Sultana, R., You, M.-H., Kondo, A., Shahpasand, K., Kim, B.M., Luo, M.-L., Nechama, M., Lin, Y.-M., 2015a. Pin1 cysteine-113 oxidation inhibits its catalytic activity and cellular function in Alzheimer's disease. Neurobiol. Dis. 76, 13–23. https://doi.org/10.1016/j.nbd.2014.12.027.
Chen, C.-H., Li, W., Sultana, R., You, M.-H., Kondo, A., Shahpasand, K., Kim, B.M., Luo, M.-L., Nechama, M., Lin, Y.-M., Yao, Y., Lee, T.H., Zhou, X.Z., Swomley, A.M., Butterfield, D.A., Zhang, Y., Lu, K.P., 2015b. Pin1 cysteine-113 oxidation inhibits its catalytic activity and cellular function in Alzheimer's disease. Neurobiol. Dis. 76, 13–23. https://doi.org/10.1016/j.nbd.2014.12.027.
Chen, D., Mei, Y., Kim, N., Lan, G., Gan, C.L., Fan, F., Zhang, T., Xia, Y., Wang, L., Lin, C., Ke, F., Zhou, X.Z., Lu, K.P., Lee, T.H., 2020a. Melatonin directly binds and inhibits death-associated protein kinase 1 function in Alzheimer's disease. J. Pineal Res. 69 (2), 12665. https://doi.org/10.1111/jpi.12665.
Chen, D., Wang, L., Lee, T.H., 2020b. Post-translational modifications of the peptidyl-prolyl isomerase Pin1. Front. Cell Dev. Biol. 8 (129), 129. https://doi.org/10.3389/fcell.2020.00129.
Deshmukh, U., Katre, P., Yajnik, C.S., 2013. Influence of maternal vitamin B12 and folate on growth and insulin resistance in the offspring. Nestle Nutr. Inst. Workshop Ser. 74, 145–154. https://doi.org/10.1159/000348463.
Driver, J.A., Lu, K.P., 2010. Pin1: a new genetic link between Alzheimer's disease, cancer and aging. Curr. Aging Sci. 3 (3), 158–165.
Dubois, B., Hampel, H., Feldman, H.H., Scheltens, P., Aisen, P., Andrieu, S., Bakardjian, H., Benali, H., Bertram, L., Blennow, K., Broich, K., Cavedo, E., Crutch, S., Dartigues, J.F., Duyckaerts, C., Epelbaum, S., Frisoni, G.B., Gauthier, S., Genthon, R., Gouw, A.A., Habert, M.O., Holtzman, D.M., Kivipelto, M., Lista, S., Molinuevo, J.L., O'Bryant, S.E., Rabinovici, G.D., Rowe, C., Salloway, S., Schneider, L.S., Sperling, R., Teichmann, M., Carrillo, M.C., Cummings, J., Jack Jr., C.R., 2016. Preclinical Alzheimer's disease: definition, natural history, and diagnostic criteria. Alzheimers Dement. 12 (3), 292–323. https://doi.org/10.1016/j.jalz.2016.02.002.
Fowler Jr., J.F., 2016. Cobalt. Dermatitis 27 (1), 3–8. https://doi.org/10.1097/der.0000000000000154.
Guan, D., Su, Y., Li, Y., Wu, C., Meng, Y., Peng, X., Cui, Y., 2015. Tetramethylpyrazine inhibits $CoCl_2$ -induced neurotoxicity through enhancement of Nrf2/GCLc/GSH and suppression of HIF1alpha/NOX2/ROS pathways. J. Neurochem. 134 (3), 551–565. https://doi.org/10.1111/jnc.13161.
Guo, Z., Tang, J., Wang, J., Zheng, F., Zhang, C., Wang, Y.L., Cai, P., Shao, W., Yu, G., Wu, S., Li, H., 2020. The negative role of histone acetylation in cobalt chloride-induced neurodegenerative damages in SHSY5Y cells. Ecotoxicol. Environ. Saf. 209, 111832 https://doi.org/10.1016/j.ecoenv.2020.111832.
Gupta, G., Gliga, A., Hedberg, J., Serra, A., Greco, D., Odnevall Wallinder, I., Fadeel, B., 2020. Cobalt nanoparticles trigger ferroptosis-like cell death (oxytosis) in neuronal cells: potential implications for neurodegenerative disease. FASEB J. 34 (4), 5262–5281. https://doi.org/10.1096/fj.201902191RR.
Hardy, J., Duff, K., Hardy, K.G., Perez-Tur, J., Hutton, M., 1998. Genetic dissection of Alzheimer's disease and related dementias: amyloid and its relationship to tau. Nat. Neurosci. 1 (5), 355–358. https://doi.org/10.1038/1565.
Herukka, S.K., Simonsen, A.H., Andreasen, N., Baldeiras, I., Bjerke, M., Blennow, K., Engelborghs, S., Frisoni, G.B., Gabryelewicz, T., Galluzzi, S., Handels, R., Kramberger, M.G., Kulczyńska, A., Molinuevo, J.L., Mroczko, B., Nordberg, A., Oliveira, C.R., Otto, M., Rinne, J.O., Rot, U., Saka, E., Soininen, H., Struyfs, H., Suardi, S., Visser, P.J., Winblad, B., Zetterberg, H., Waldemar, G., 2017. Recommendations for cerebrospinal fluid Alzheimer's disease biomarkers in the diagnostic evaluation of mild cognitive impairment. Alzheimers Dement. 13 (3), 285–295. https://doi.org/10.1016/j.jalz.2016.09.009.
Hong, X., Liu, C., Momotaz, H., Cassidy, K., Sajatovic, M., Sahoo, S.S., 2019. Enhancing multi-center patient cohort studies in the managing epilepsy well (MEW) network: integrated data integration and statistical analysis. AMIA Annu Symp. Proc. 2019, 1071–1080.
International AsD, 2019. World Alzheimer Report 2019: Attitudes to Dementia. Alzheimer's Disease International (ADI), London, UK. ⟨https://www.alz.co.uk/research/WorldAlzheimerReport2019.pdf⟩.
Kondo, A., Shahpasand, K., Mannix, R., Qiu, J., Moncaster, J., Chen, C.-H., Yao, Y., Lin, Y.-M., Driver, J.A., Sun, Y., 2015. Antibody against early driver of neurodegeneration cis P-tau blocks brain injury and tauopathy. Nature 523 (7561), 431–436. https://doi.org/10.1038/nature14658.
Lanni, C., Masi, M., Racchi, M., Govoni, S., 2020. Cancer and Alzheimer's disease inverse relationship: an age-associated diverging derailment of shared pathways. Mol. Psychiatry 26, 280–295. https://doi.org/10.1038/s41380-020-0760-2.
Lee, M.-S., Kao, S.-C., Lemere, C.A., Xia, W., Tseng, H.-C., Zhou, Y., Neve, R., Ahlijanian, M.K., Tsai, L.-H., 2003. APP processing is regulated by cytoplasmic phosphorylation. J. Cell Biol. 163 (1), 83–95. https://doi.org/10.1083/jcb.200301115.
Lee, T.H., Pastorino, L., Lu, K.P., 2011. Peptidyl-prolyl cis–trans isomerase Pin1 in ageing, cancer and Alzheimer disease. Expert Rev. Mol. Med. 13, 21. https://doi.org/10.1017/S1462399411001906.
Léonard, A., Lauwerys, R., 1990. Mutagenicity, carcinogenicity and teratogenicity of cobalt metal and cobalt compounds. Mutat. Res. 239 (1), 17–27. https://doi.org/10.1016/0165-1110(90)90029-b.
Leyssens, L., Vinck, B., Van Der Straeten, C., Wuyts, F., Maes, L., 2017. Cobalt toxicity in humans—a review of the potential sources and systemic health effects. Toxicology 387, 43–56. https://doi.org/10.1016/j.tox.2017.05.015.
Liao, Y., Wei, Y., Zhou, X., Yang, J.Y., Dai, C., Chen, Y.J., Agarwal, N.K., Sarbassov, D., Shi, D., Yu, D., Hung, M.C., 2009. Peptidyl-prolyl cis/trans isomerase Pin1 is critical for the regulation of PKB/Akt stability and activation phosphorylation. Oncogene 28 (26), 2436–2445. https://doi.org/10.1038/onc.2009.98.
Liou, Y.-C., Ryo, A., Huang, H.-K., Lu, P.-J., Bronson, R., Fujimori, F., Uchida, T., Hunter, T., Lu, K.P., 2002a. Loss of Pin1 function in the mouse causes phenotypes resembling cyclin D1-null phenotypes. Proc. Natl. Acad. Sci. USA 99 (3), 1335–1340.
Liou, Y.-C., Ryo, A., Huang, H.-K., Lu, P.-J., Bronson, R., Fujimori, F., Uchida, T., Hunter, T., Lu, K.P., 2002b. Loss of Pin1 function in the mouse causes phenotypes resembling cyclin D1-null phenotypes. Proc. Natl. Acad. Sci. USA 99 (3), 1335–1340. https://doi.org/10.1073/pnas.032404099.
Lison, D., van den Brule, S., Van Maele-Fabry, G., 2018. Cobalt and its compounds: update on genotoxic and carcinogenic activities. Crit. Rev. Toxicol. 48 (7), 522–539. https://doi.org/10.1080/10408444.2018.1491023.
Lu, K.P., Liou, Y.C., Vincent, I., 2003. Proline-directed phosphorylation and isomerization in mitotic regulation and in Alzheimer's Disease. BioEssays 25 (2), 174–181. https://doi.org/10.1002/bies.10223.
Lu, P.-J., Wulf, G., Zhou, X.Z., Davies, P., Lu, K.P., 1999. The prolyl isomerase Pin1 restores the function of Alzheimer-associated phosphorylated tau protein. Nature 399 (6738), 784–788. https://doi.org/10.1038/21650.
Maliha, A.M., Kuehn, S., Hurst, J., Herms, F., Fehr, M., Bartz-Schmidt, K.U., Dick, H.B., Joachim, S.C., Schnichels, S., 2019. Diminished apoptosis in hypoxic porcine retina explant cultures through hypothermia. Sci. Rep. 9 (1), 4898. https://doi.org/10.1038/s41598-019-41113-4.
Manolio, T.A., Collins, F.S., Cox, N.J., Goldstein, D.B., Hindorff, L.A., Hunter, D.J., McCarthy, M.I., Ramos, E.M., Cardon, L.R., Chakravarti, A., 2009. Finding the missing heritability of complex diseases. Nature 461 (7265), 747–753. https://doi.org/10.1038/nature08494.
Massagué, J., 2004. G1 cell-cycle control and cancer. Nature 432 (7015), 298–306. https://doi.org/10.1038/nature03094.
Ma, S.L., Tang, N.L., Tam, C.W., Cheong Lui, V.W., Lam, L.C., Chiu, H.F., Driver, J.A., Pastorino, L., Lu, K.P., 2012. A PIN1 polymorphism that prevents its suppression by AP4 associates with delayed onset of Alzheimer's disease. Neurobiol. Aging 33, 804–813. https://doi.org/10.1016/j.neurobiolaging.2010.05.018.
Mattson, M.P., 2004. Pathways towards and away from Alzheimer's disease. Nature 430 (7000), 631–639. https://doi.org/10.1038/nature02621.
Muñoz-Sánchez, J., Chánez-Cárdenas, M.E., 2019. The use of cobalt chloride as a chemical hypoxia model. J. Appl. Toxicol. 39 (4), 556–570. https://doi.org/10.1002/jat.3749.
Nakamura, K., Greenwood, A., Binder, L., Bigio, E.H., Denial, S., Nicholson, L., Zhou, X. Z., Lu, K.P., 2012. Proline isomer-specific antibodies reveal the early pathogenic tau conformation in Alzheimer's disease. Cell 149 (1), 232–244. https://doi.org/10.1016/j.cell.2012.02.016.
Olivieri, G., Hess, C., Savaskan, E., Ly, C., Meier, F., Baysang, G., Brockhaus, M., Müller-Spahn, F., 2001a. Melatonin protects SHSY5Y neuroblastoma cells from cobalt-induced oxidative stress, neurotoxicity and increased β-amyloid secretion. J. Pineal Res. 31 (4), 320–325.
Olivieri, G., Hess, C., Savaskan, E., Ly, C., Meier, F., Baysang, G., Brockhaus, M., Muller-Spahn, F., 2001b. Melatonin protects SHSY5Y neuroblastoma cells from cobalt-induced oxidative stress, neurotoxicity and increased beta-amyloid secretion. J. Pineal Res. 31 (4), 320–325. https://doi.org/10.1034/j.1600-079x.2001.310406.x.
Park, J.S., Lee, J., Jung, E.S., Kim, M.H., Kim, I.B., Son, H., Kim, S., Kim, S., Park, Y.M., Mook-Jung, I., Yu, S.J., Lee, J.H., 2019. Brain somatic mutations observed in Alzheimer's disease associated with aging and dysregulation of tau phosphorylation. Nat. Commun. 10 (1), 3090. https://doi.org/10.1038/s41467-019-11000-7.
Pastorino, L., Sun, A., Lu, P.-J., Zhou, X.Z., Balastik, M., Finn, G., Wulf, G., Lim, J., Li, S.-H., Li, X., 2006. The prolyl isomerase Pin1 regulates amyloid precursor protein processing and amyloid-β production. Nature 440 (7083), 528–534. https://doi.org/10.1038/nature04543.
Paustenbach, D.J., Tvermoes, B.E., Unice, K.M., Finley, B.L., Kerger, B.D., 2013. A review of the health hazards posed by cobalt. Crit. Rev. Toxicol. 43 (4), 316–362. https://doi.org/10.3109/10408444.2013.779633.
Phiel, C.J., Wilson, C.A., Lee, V.M.-Y., Klein, P.S., 2003. GSK-3α regulates production of Alzheimer's disease amyloid-β peptides. Nature 423 (6938), 435–439. https://doi.org/10.1038/nature01640.
Risal, P., Park, B.-H., Cho, B.H., Kim, J.-C., Jeong, Y.J., 2012. Overexpression of peptidyl-prolyl isomerase Pin1 attenuates hepatocytes apoptosis and secondary necrosis

following carbon tetrachloride-induced acute liver injury in mice. Pathol. Int. 62 (1), 8–15. https://doi.org/10.1111/j.1440-1827.2011.02744.x.

Shaw, L.M., Korecka, M., Figurski, M., Toledo, J., Irwin, D., Hee Kang, J., Trojanowski, J. Q., 2020. Detection of Alzheimer disease pathology in patients using biochemical biomarkers: prospects and challenges for use in clinical practice. J. Appl. Lab. Med. 5 (1), 183–193. https://doi.org/10.1373/jalm.2019.029587.

Sherzai, A.Z., Parasram, M., Haider, J.M., Sherzai, D., 2020. Alzheimer disease and cancer: a national inpatient sample analysis. Alzheimer Dis. Assoc. Disord. 34 (2), 122–127. https://doi.org/10.1097/WAD.0000000000000369.

Sidaginamale, R.P., Joyce, T.J., Lord, J.K., Jefferson, R., Blain, P.G., Nargol, A.V., Langton, D.J., 2013. Blood metal ion testing is an effectivescreening tool to identify poorly performing metal-on-metal bearingsurfaces. Bone Jt. Res. 2 (5), 84–95. https://doi.org/10.1302/2046-3758.25.2000148.

Song, F., Poljak, A., Valenzuela, M., Mayeux, R., Smythe, G.A., Sachdev, P.S., 2011. Meta-analysis of plasma amyloid-beta levels in Alzheimer's disease. J. Alzheimers Dis. 26 (2), 365–375. https://doi.org/10.3233/jad-2011-101977.

Sultana, R., Boyd-Kimball, D., Poon, H.F., Cai, J., Pierce, W.M., Klein, J.B., Markesbery, W.R., Zhou, X.Z., Lu, K.P., Butterfield, D.A., 2006. Oxidative modification and down-regulation of Pin1 in Alzheimer's disease hippocampus: a redox proteomics analysis. Neurobiol. Aging 27 (7), 918–925. https://doi.org/10.1016/j.neurobiolaging.2005.05.005.

Sun, R., Wang, H., Shi, Y., Sun, Z., Jiang, H., Zhang, J., 2020. Changes in the morphology, number, and pathological protein levels of plasma exosomes may help diagnose Alzheimer's disease. J. Alzheimers Dis. 73 (3), 909–917. https://doi.org/10.3233/jad-190497.

Tang, J., Zheng, C., Zheng, F., Li, Y., Wang Y-l, Aschner, M., Guo, Z., Yu, G., Wu, S., Li, H., 2020a. Global N6-methyladenosine profiling of cobalt-exposed cortex and human neuroblastoma H4 cells presents epitranscriptomics alterations in neurodegenerative disease-associated genes. Environ. Pollut. 266, 115326 https://doi.org/10.1016/j.envpol.2020.115326.

Tang, J., Zheng, C., Zheng, F., Li, Y., Wang, Y.L., Aschner, M., Guo, Z., Yu, G., Wu, S., Li, H., 2020b. Global N6-methyladenosine profiling of cobalt-exposed cortex and human neuroblastoma H4 cells presents epitranscriptomics alterations in neurodegenerative disease-associated genes. Environ. Pollut. 266 (Pt 2), 115326 https://doi.org/10.1016/j.envpol.2020.115326.

Tvermoes, B.E., Paustenbach, D.J., Kerger, B.D., Finley, B.L., Unice, K.M., 2015. Review of cobalt toxicokinetics following oral dosing: implications for health risk assessments and metal-on-metal hip implant patients. Crit. Rev. Toxicol. 45 (5), 367–387. https://doi.org/10.3109/10408444.2014.985818.

Van Der Straeten, C., Van Quickenborne, D., De Roest, B., Calistri, A., Victor, J., De Smet, K., 2013. Metal ion levels from well-functioning Birmingham Hip Resurfacings decline significantly at ten years. Bone Jt. J. 95-b (10), 1332–1338. https://doi.org/10.1302/0301-620x.95b10.32022.

Wang, J., Liu, K., Wang, X.F., Sun, D.J., 2017. Juglone reduces growth and migration of U251 glioblastoma cells and disrupts angiogenesis. Oncol. Rep. 38 (4), 1959–1966. https://doi.org/10.3892/or.2017.5878.

Wei, S., Kozono, S., Kats, L., Nechama, M., Li, W., Guarnerio, J., Luo, M., You, M.H., Yao, Y., Kondo, A., Hu, H., Bozkurt, G., Moerke, N.J., Cao, S., Reschke, M., Chen, C. H., Rego, E.M., Lo-Coco, F., Cantley, L.C., Lee, T.H., Wu, H., Zhang, Y., Pandolfi, P.P., Zhou, X.Z., Lu, K.P., 2015. Active Pin1 is a key target of all-trans retinoic acid in acute promyelocytic leukemia and breast cancer. Nat. Med. 21 (5), 457–466. https://doi.org/10.1038/nm.3839.

Wenstrup, D., Ehman, W.D., Markesbery, W.R., 1990. Trace element imbalances in isolated subcellular fractions of Alzheimer's disease brains. Brain Res. 533 (1), 125–131. https://doi.org/10.1016/0006-8993(90)91804-p.

Wu, Z., Zhang, M., Zhang, Z., Dong, W., Wang, Q., Ren, J., 2018. Ratio of beta-amyloid protein (Abeta) and Tau predicts the postoperative cognitive dysfunction on patients undergoing total hip/knee replacement surgery. Exp. Ther. Med. 15 (1), 878–884. https://doi.org/10.3892/etm.2017.5480.

Zheng, F., Chen, P., Li, H., Aschner, M., 2020. Drp-1 dependent mitochondrial fragmentation contributes to cobalt chloride induced toxicity in Caenorhabditis elegans. Toxicol. Sci. 177, 158–167. https://doi.org/10.1093/toxsci/kfaa105.

Zheng, F., Luo, Z., Zheng, C., Li, J., Zeng, J., Yang, H., Chen, J., Jin, Y., Aschner, M., Wu, S., 2019. Comparison of the neurotoxicity associated with cobalt nanoparticles and cobalt chloride in Wistar rats. Toxicol. Appl. Pharmacol. 369, 90–99. https://doi.org/10.1016/j.taap.2019.03.003.